Naval Research Laboratory

Stennis Space Center, MS 39529-5004

NRL/MR/7320--12-9425

Validation Test Report for WAVEWATCH III

W. Erick Rogers
James D. Dykes
David Wang

Ocean Dynamics and Prediction Branch
Oceanography Division

Suzanne N. Carroll
Kim Watson

QinetiQ North America
Slidell, Louisiana

November 30, 2012

REPORT DOCUMENTATION PAGE

Form Approved
OMB No. 0704-0188

1. REPORT DATE *(DD-MM-YYYY)*	**2. REPORT TYPE**	**3. DATES COVERED** *(From - To)*
30-11-2012	Memorandum Report	

4. TITLE AND SUBTITLE

Validation Test Report for WAVEWATCH III

5a. CONTRACT NUMBER

5b. GRANT NUMBER

5c. PROGRAM ELEMENT NUMBER
0603207N

6. AUTHOR(S)

W. Erick Rogers, James D. Dykes, David Wang, Suzanne N. Carroll,[1] and Kim Watson[1]

5d. PROJECT NUMBER

5e. TASK NUMBER

5f. WORK UNIT NUMBER
73-5097-A3-5

7. PERFORMING ORGANIZATION NAME(S) AND ADDRESS(ES)

Naval Research Laboratory
Oceanography Division
Stennis Space Center, MS 39529-5004

8. PERFORMING ORGANIZATION REPORT NUMBER

NRL/MR/7320--12-9425

9. SPONSORING / MONITORING AGENCY NAME(S) AND ADDRESS(ES)

Space & Naval Warfare Systems Command
2451 Crystal Drive
Arlington, VA 22245-5200

10. SPONSOR / MONITOR'S ACRONYM(S)

SPAWAR

11. SPONSOR / MONITOR'S REPORT NUMBER(S)

12. DISTRIBUTION / AVAILABILITY STATEMENT

Approved for public release; distribution is unlimited.

13. SUPPLEMENTARY NOTES

[1]QinetiQ North America, Slidell, LA 70461

14. ABSTRACT

This document serves as the Validation Test Report for the WAVEWATCH III model transition to the Naval Oceanographic Office (NAVOCEANO). A literature review is given, focusing on prior validation efforts, such as those by FNMOC and NCEP comparing WAM and WAVEWATCH III. An experimental realtime system is now running on NAVOCEANO hardware and uses the "multi-grid" (two-way nesting) feature of WW3, with a global grid and nine regional grids. The realtime system is validated in a limited sense using several coastal and deep-water NOAA NDBC buoys. The third component provides a thorough validation. This is done using a single-grid global wave model hindcast for the last four months of 2010. The primary "ground truth" for this section is satellite altimetry, though several deep-water buoys are also used here. Four hindcasts are evaluated, using two alternate forms of wave model physics. In a final section, recommendations for the future are given.

15. SUBJECT TERMS

WAVEWATCH III
Wave model
Windsea
Swell

16. SECURITY CLASSIFICATION OF:			**17. LIMITATION OF ABSTRACT**	**18. NUMBER OF PAGES**	**19a. NAME OF RESPONSIBLE PERSON**
a. REPORT	**b. ABSTRACT**	**c. THIS PAGE**			W. Erick Rogers
Unclassified Unlimited	Unclassified Unlimited	Unclassified Unlimited	Unclassified Unlimited	73	**19b. TELEPHONE NUMBER** *(include area code)* 228-688-4727

TABLE OF CONTENTS

FIGURES AND TABLES

1.0 INTRODUCTION

Contributing authors: Suzanne Carroll, Kim Watson

This Validation Test Report serves as documentation to accompany the transition of the WAVEWATCH III® model to the Naval Oceanographic Office (NAVOCEANO), replacing the WAM model being used there now for all large-scale modeling of wind-generated surface gravity waves.

1.1 WAVEWATCH III®

WAVEWATCH III® (Tolman 1997, 1999a, 2009) is a third generation wave model developed at NOAA/NCEP from the example of the WAM model (WAMDIG 1988, Komen *et al*. 1994). It began as WAVEWATCH, a Delft University of Technology (Tolman 1989, 1991) model and evolved into WAVEWATCH II, developed at NASA, Goddard Space Flight Center (e.g., Tolman 1992). WW3 solves the random phase spectral action density balance equation for wave number-direction spectra, the implicit assumption of this equation being that properties of water depth and current, as well as the wave field itself, differ on space and time scales that are much larger than the variation scales of a single wave. With version 3.14 some source term options for extremely shallow water (surf zone) are included. Whereas the surf-zone physics implemented in earlier versions have been quite rudimentary, the wave model can now be applied to any areas of shallow water selected at random.

WAVEWATCH III® represents quite a departure from its predecessors with respect to its governing equations, numerical methods, model structure, and physical parameterizations. The governing equations include refraction and straining of the wave field due to spatial and temporal variations of the mean water depth and mean current (tides, surges etc.), where applicable. Wave propagation is linear, and applicable nonlinear effects are included in the physics. The model allows dynamically updated ice coverage and spectral partitioning for post-processing of point output (or for the entire wave model grid) using the Vincent and Soille (1991) algorithm (Hanson and Jenssen, 2004; Hanson et al., 2006, 2009). WAVEWATCH III® includes several methods to alleviate the Garden Sprinkler Effect (Booij and Holthuijsen, 1987, Tolman, 2002b). Also included in version 3.14 is sub-grid representation of unresolved islands (Tolman 2002e). An automated grid generation package based on MATLAB® has been developed to automate the generation of grids, including obstructions due to unresolved islands (Chawla and Tolman, 2007, 2008). WAVEWATCH III® has parameterizations of physical processes (source terms) such as wave growth and decay due to wind action, nonlinear resonant interactions, bottom friction, dissipation ('whitecapping'), surf-breaking (i.e., depth-induced breaking) and scattering due to wave-bottom interactions. The model is prepared for triad interactions. For deepwater physics, prior versions of WAVEWATCH III® included WAM cycle 3 physics and Tolman and Chalikov (1996) physics. This latest version, version 3.14, contains WAM cycle 4 physics as well. Wetting and drying is accommodated within the model. In this latest release, WAVEWATCH III® has progressed from simply a wave model to a wave modeling framework in which additional physical and numerical techniques may be developed.

Manuscript approved July 6, 2012.

1.2 Multi-Grid WAVEWATCH III®

WAVEWATCH III® version 3.14 has the option of using a "mosaic" grid configuration, where an arbitrary number of grids can be incorporated into a run with full two-way interactions between all grids. The mosaic of grids then operates as a single model with variable spatial resolution (Tolman, 2006, 2007, 2008). Single-grid simulations may move along a user-defined path, allowing for a shifting of the grid to follow hurricanes, for example (Tolman and Alves, 2005). The multi-grid configuration considers only static grids as yet, but the ability to consider moving grids within the mosaic is being developed.

1.3 Software Design

WAVEWATCH III® is fully modular and dynamically allocated, coded in ANSI standard FORTRAN 90. The model can optionally be compiled to include shared memory parallelisms using OpenMP compiler directives. It may also be compiled for a distributed memory environment using the Message Passing Interface (MPI, see Tolman 2002c).

WAVEWATCH III® grids may be either Cartesian or regularly spaced longitude-latitude grids, where the latitude and longitude increments need not be equal. The model can be set up for traditional one-way nesting, where grids are run as separate systems consecutively, starting with the lowest spatial resolution models. It can also use the multi-grid system described above.

Both first order accurate and third order accurate numerical schemes are available to describe wave propagation (Tolman 1995). The propagation scheme is selected at the compile level. Wave energy spectra are discretized through a constant directional increment (spanning all directions) and a spatially varying wave number grid. The latter grid relates to an invariant logarithmic intrinsic frequency grid (Tolman and Booij 1998). The source terms are integrated in time through a dynamically adjusted time stepping algorithm, which permits more frequent computations during conditions with rapid spectral changes (Tolman 1992, 1997, 1999a, 2009).

There are several options for model output. WAVEWATCH III® version 4 writes up to 1000 restart files per model run. The model provides binary and ASCII output, as well as output for the Grid Analysis and Display System (GrADS) graphics package during post processing. Postprocessors for Gridded Binary (GRIB) data are also available but require GRIB packing libraries.

The user may specify output of wave spectra at selected locations or along arbitrary tracks. Partitioned wave field information is available for the full model grid or sub-sets and sub-sampled grids. Gridded fields of 31 input and mean wave parameters are available, such as significant wave height, directions, and frequencies. The model contains boundary data files for up to nine separate nested runs through a one-way nested model approach where models are run independently. In the mosaic approach, input boundary data for each grid in the mosaic can be dumped for later use.

As WAVEWATCH III® is updated and improved, so is the software design. Therefore, in-line documentation is included throughout the model code and is updated as the code is updated. In addition to source code, the National Centers for Environmental Prediction (NCEP) code

repository includes test cases, stencil files for model instructions, a manual, and a build system. Thus, the user manual is updated in step with code changes.

1.4 Document Overview

The objective of this report is to document validation of the WAVEWATCH III® (WW3) model. Of primary concern is the skill of the real-time system implemented at the Naval Oceanographic Office (NAVOCEANO). However, it is not necessary to rely exclusively on direct comparison of the real-time system to observations. Here we use two additional strategies: first, we exploit prior validation studies using this model, of which there are many. Second, we apply the model in a hindcast (i.e. not real-time) that is intended to capture the main features of the real-time system.

Section 2 summarizes earlier validation studies by both Navy and non-Navy researchers, evaluating and comparing WW3 and WAM performance using buoy and altimeter observational data.

In Section 3, the real-time implementation of the multi-grid WW3 system is presented. Direct comparison to observational data is included in this section, limited to comparing model output significant wave height to observations from buoys surrounding the North American continent of which five are presented in the body of the section and the results of several more are included in the appendix. No altimeter data were used. As such, the comparisons serve to simply verify consistency of the model with implications of some skill improvement of WW3 over WAM even in shallow water regions and coastal waters. Highlights of the technical aspects of real-time implementation of the model at NAVOCEANO are also provided in Section 3.

In Section 4, a four-month duration global, single-grid hindcast is presented. The significant wave height (SWH) predictions from this hindcast are comprehensively compared with altimeter data. These satellite observations are the primary source of ground truth in this section, but wave height observations from four buoys are also included.

Some features of these historical validation studies (Section 2) are much more comprehensive than the new validations presented in Sections 3 and 4. For example, some studies utilize dozens of buoys, and some studies evaluate the accuracy of the wave model for prediction of quantities derived from the wave spectrum besides the lowest order quantity, wave height.

The procedures and results of validating the WW3 system are detailed. A description of the purpose of each test, the test area characteristics, model run specifics, and results from each simulation will be presented here, along with graphical output, statistics, and concluding remarks. The user can refer to the WAVEWATCH III® User's Guide (Tolman et al., 2009) for further information on the model. Online documentation is available for the latest version of WW3. It may be found at the NCEP website:
http://polar.ncep.noaa.gov/waves/wavewatch/
and http://polar.ncep.noaa.gov/mmab/papers/tn276/MMAB_276.pdf

2.0 PREVIOUS WAVEWATCH III® VALIDATION EFFORTS

Contributing authors: Suzanne Carroll, Kim Watson

Several validation studies have been conducted over the years as WW3 has evolved to its current version 3.14. These have compared earlier versions of WW3 to WAM in various versions and applications as well as to buoy and altimetry data in global and regional applications. The validations experiments have been conducted in both non-Navy and Navy environments. Table 2-1 summarizes the findings of the non-Navy articles and Table 2-2 gives an overview of Navy validation studies for WW3.

Before starting, we clarify our references to the physics of WW3. In early versions of the model (2.22 and earlier), there were only two deepwater physics packages available. These were ST1 and ST2, where ST1 is WAM Cycle 3 physics (Komen et al. 1984; WAMDI Group 1988) and ST2 is the deepwater physics of Tolman and Chalikov (1996) (or TC96). Whenever early documents refer to the deepwater physics of WW3, this is specifically TC96. In later versions, ST3 and ST4 are additional options: both are described in Ardhuin et al. 2010. Thus, in applications of later versions, we are explicit with regard to the physics package used.

Table 2-1 and Table 2-2 include information on some model settings. All WW3 simulations described in these tables used default WW3 physics (TC 96) and the third-order "ULTIMATE QUICKEST" (UQ) propagation scheme.

2.1 Non-Navy Validation Studies

2.1.1 Validation of WW3 v. 1.15 for a Global Domain (Tolman, 2002a)

In this study, WW3 version 1.15, was evaluated for its success in providing global wave hindcasts in an operational environment. The model required some initial tuning and modifications to the swell-to-atmosphere interactions. Mean currents and water level variations were ignored in this global application. Some shallow water effects were included (refraction, shoaling, bottom friction), although they are fairly irrelevant on a global grid. The input and dissipation source term parameterization was that of TC96 with modifications. WW3 used the third-order "ULTIMATE QUICKEST" (UQ) propagation scheme (Leonard, 1979, 1991) with a correction for the description of continuous dispersion in a discrete spectral model as detailed in Tolman (1995).

WW3 was setup with a longitude-latitude grid from 78° N to 78° S, a resolution of 1.25° x 1°, and a minimum water depth of 25 m. The discrete spectrum had 24 directions and 25 frequencies ranging from 0.042 Hz to 0.41 Hz. Ten meter winds came from the NCEP's Global Data Assimilation System (GDAS). If sea-ice concentrations exceeded 33% the grid points were treated as land. The model uses four time steps. The first is the time increment at which the total solution is propagated and the input wind field was interpolated, as well as the maximum time step in the source term integration. The second is the maximum propagation time step for the longest wave components in a spectrum. The third time step is for refraction. The last time step is the minimum for source term integration. In this global hindcast, the four time steps were set to 3600, 1300, 3600, and 300 seconds, respectively. The model was re-tuned

to remove systemic biases by characterizing an effective wind speed internal to the model. This gave reasonable results in closed basins and in storm tracks at higher latitudes but an underestimation at tropical latitudes. WAM cycle 4 was run with the same spatial and spectral grids and wind input as WW3. The time step for WAM was 1200 seconds. Ice coverage was not included in WAM simulations.

The observations used in validating the model results came from buoy data and satellite altimetry. There were 29 buoys from the World Meteorological Organization using Geostationary Operational Environmental Satellites (GOES) and World Meteorological Organization (WMO) Global Telecommunication System (GTS) transmissions to validate the global WW3 and WAM models in wave spectra and wave height. However, buoy data covers only small parts of the oceans, rendering them only partially effective in global model validation. Satellite altimetry from the European Remote Sensing satellite 1 (ERS-1) was the primary source for ground truth in this study. The ERS-1 footprint was 6.5 km and the data was averaged over 10 s intervals, resulting in an effective footprint of 6.5 x 65 km^2.

WW3 performed well overall in comparisons to altimeter and buoy data. The normalized total model error, also known as the scatter index (SI) is the root mean square error (RMSE) normalized with the mean observed value. The WW3 and WAM wave models with scatter indices of ~15% are considered successful forecast systems. WW3 RMSE was less than 15% of the mean observed wave heights for almost the entire global domain. Scatter indices for WAM cycle 4 were higher, greater than 0.20 for large areas in tropical waters. The WW3 model outperformed WAM with regard to swell prediction in tropical regions, in wave height prediction, and in the distribution of extreme events. Random errors for wave height with WW3 ranged from 0.3-0.4 m for low wave heights and 0.15 m for higher waves. WW3 did not perform as well as WAM in high latitude areas of the global domain. Tolman reports that WW3 cannot achieve good growth characteristics for both fetch-limited and open ocean conditions with a single source term calibration and claims that this characteristic is shared by WAM[1]. WW3 biases were smaller than in WAM and essentially randomly distributed across the global grid domain. The model underestimated the highest waves and overestimated the lowest waves. WW3 more closely reproduced observed wave height distributions. When compared to buoy data in the NE Atlantic, WAM showed smaller RMS errors in regions of high latitude and smaller biases and RMS errors for extreme wave heights. The RMS errors of WW3 were much smaller in the tropics. It must be noted that WAM had been tuned more to buoy data for a longer period of time and WW3 tuned to altimeter data, even to data in the present study. The tuning of these models led to altimetry data that more closely matched WW3 than buoy data. However, WW3 also verified well with buoy data, which played a minor role in its tuning.

[1] This is consistent with our experience applying the TC96 physics. Accuracy with the default calibration is quite good for basin-scale applications such as the Gulf of Mexico, but the same calibration is inaccurate for smaller scales such as the Great Lakes (e.g. Ardhuin et al. 2010). We have not noticed any such problem using the WAM4 physics as implemented in WW3 version 3.14. However, keep in mind that Tolman (2002a) was using WAM itself, rather than WAM4 physics in WW3. Therefore, we do not dispute the claim by Tolman (2002a) that this negative characteristic is shared by WAM.

2.1.2 NOAA's global WW3 (NWW3) (WW3 v. 1.15) comparison with other NCEP ocean surface wave models (Tolman et al., 2002)

This study compared the NOAA global WW3 system (NWW3) with the WAM model in several of the world's oceans. The NWW3 wave model was set up with a 1° x 1.25° spatial resolution on a grid ranging from 78° N to 78° S with 288 x 157 grid points. The global time step was 3600 s. The spectrum was discretized with 24 directions at a 15° increment and 25 frequencies, ranging from 0.041 to 0.42 Hz with a 10% increment. The physics parameterizations were set to default WW3 settings.

The NWW3 wave model was forced with winds and temperatures from GDAS (Kanamitsu 1989; Derber et al. 1991) and from the operational Medium-Range Forecast system (MRF; Kanamitsu 1989; Kanamitsu et al. 1991; Caplan et al. 1997), which are available at 3-h intervals. For all but the first 12 days of the study, the resolution was set to T170 with 42 levels. Daily ice concentrations came from NCEP's automated passive microwave sea ice concentration analysis (Grumbine 1996).

The models were validated against NOAA NDBC fixed buoy observations and ERS-2 altimeter data. All buoys were located in the Northern Hemisphere and did not cover the deep ocean well. The buoy data were quality controlled manually at NCEP's Ocean Modeling Branch (OMB). Both significant wave height and wind data from buoys were used. As in Tolman (1998b), fast-delivery ERS-2 data were retrieved from the operational data flow at NCEP and averaged along the track in 10-s intervals at scales comparable to the wave models. The parallel comparison and validation period began 12 January 1998 and ended 30 June 1998.

In hindcast wave height time series at selected buoys, NWW3 resolved maximum and minimum wave heights better than WAM, particularly for swells around Hawaii and in the Gulf of Mexico. Bulk statistical comparisons to buoy observations suggested that NWW3 could be too energetic, always overestimating wave heights (regression slopes) by about 10%. WAM generally underestimated regression slopes by about 7%, despite the lack of sheltering by islands. Excessively high regression slopes of NWW3 near Hawaii (1.343 vs. WAM's 0.891) were clearly due to a lack of proper sheltering of several buoys by the islands in the model. In a joint SWH comparison to buoys for a 24 hr forecast near Hawaii, the correlation coefficient for NWW3 was 0.870 and for WAM it was 0.766. Near Japan the regression slope for a 24 hr forecast was 0.953 compared to WAM's slope of 0.701. Regional comparisons of both models to buoy data showed much larger differences, with generally better model behavior for NWW3.

Because NWW3 has a more responsive nature[2], it is more sensitive to errors in the wind forecasts, showing more rapid error growth with forecast time than WAM. High regression slopes in NWW3 may suggest that error growth rates in NWW3 are too large, and they may be driven either by NWW3's responsive nature or by the lack of sheltering in certain cases. The

[2] "More responsive" as used here presumably refers to the larger variance in WW3 comparisons—both in time series and in spatial presentations—relative to WAM. This is at least partially attributable to the diffusive propagation scheme used by WAM. However, the TC96 source terms are weaker in general than those of WAM, so in that sense WW3 may be expected to be *less* responsive to changes in forcing than WAM (i.e. longer relaxation times); for further discussion, see Ardhuin et al. (2007).

present data cannot definitively isolate the source of the overestimation of the regression coefficient in NWW3. Because the regression coefficient in WAM is too low, except in cases of extreme lack of sheltering, the error growth rates in WAM are too low.

Both systems were also validated against altimeter data. The comparisons at higher northern latitudes were very similar to those against all buoy data, with WAM showing less bias (NWW3 bias = 0.11, WAM = -0.04). In the Tropics and in the Southern Hemisphere (South of 30°S), NWW3 performed better than WAM (NWW3 bias = 0.10; WAM bias =-0.17). Both models showed alternate areas with positive and negative biases in the range of -0.5 to 0.5 m.

2.1.3 WW3 v. 2.22 with wind generated waves from Hurricane Isabel (Tolman et al., 2004)

Hurricane Isabel hit the east coast of the US in September 2003 with significant wave heights measured by National Data Buoy Center (NDBC) buoys at > 10 m approximately 250 nm offshore. The WW3 suite of models was validated in this study, which consisted of a global model of resolution 1° x 1.25° in lat/lon and several regional models with 0.25° spatial resolutions (Tolman et al, 2002c, Chen et al., 2003). The North Atlantic Hurricane wave model (NAH) and the Western North Atlantic regional wave model (WNA), both based on version 2.22 of WW3, provided the hurricane wave predictions for the period of September 6 through 19, 2003. Wind forcing for the WNA wave model came from 3-hourly analysis and forecast winds of the Global Forecasting System (GFS) model (Caplan et al., 1997). The NAH wave model used hourly high resolution winds from the Geophysical Fluid Dynamics Laboratory (GFDL) model blended with the GFS winds through the blending scheme of Chao and Tolman (2000, 2001).

Ice for the wave models input consisted of ice concentration fields from NCEP's automated passive microwave sea ice concentration analysis (Grumbine, 1996). Wind field quality was assessed through analysis performed by the Atlantic Oceanographic and Meteorological Laboratory (AOML). Storm intensity, in the WNA and NAH models, was evaluated by comparing maximum wind speeds in both models with maximum AOML wind speed analyses. This study undertook extensive analysis of the quality of these wind fields.

Observational wave height and spectral data used in this validation came from 15 NDBC buoys as well as Jason-1 satellite altimeter data. The satellite altimetry data included four passes through or near the eye of Isabel. The buoy data provided useful significant wave height comparisons when Isabel approached land, but the Jason-1 altimetry allowed for more accurate assessments of model performance with respect to extreme wave conditions throughout Isabel's journey through the Gulf of Mexico, in both deep water and at the coast.

For both NAH and WNA wind fields, forecast maximum wind speeds were lower than hindcast maximum winds. This appeared to be the case when Isabel was most intense and relatively small. The forecast wind speeds were more accurate near landfall, when Isabel was less intense but larger. Both models provided excellent forecasts for Isabel just before the storm made landfall, but the NAH model outperformed the WNA model in Isabel's early stages as a category 5 hurricane. The NAH model more accurately predicted swell along the east coast prior to the storm's landfall. Most of the model's shortcomings are attributed to the driving

wind fields. In comparing both models to buoy data, the NAH model had lower scatter indices than the WNA model at all but three of the 15 buoy locations. When compared to Jason-1 altimetry data during the early and most intense part of Isabel's life cycle, the WNA severely underestimated wave heights. The NAH showed improvement but overestimated maximum wave heights. Swell generated by the NAH model agreed more closely with observations than the WNA model, which could be attributed to the GFS wind field quality.

For a ten day period of hindcast comparisons to mean wave height from buoys, biases were low for both models. The RMS errors and scatter indices were typical for event analyses but larger than most normal model validations over long time frames. The NAH model, the WW3 model designed for hurricane wave prediction, outperformed the WNA model statistically. Both models provided good forecasts for Isabel near landfall for the 72 hr NAH forecast and for many more days for the WNA model. At buoy 41025, which is closest to where Isabel made landfall, the NAH model had wave height biases of -0.01, and RMSE of 0.68, and a SI of 23%. At the same buoy, the WNA model had a bias of -0.35, an RMSE of 0.80, and a SI of 27%. Most model deficiencies are related to wind field deficiencies used to force the models. The WW3 v2.22 model needed improvements in shallow water, in physical parameterizations for extreme wind events, in wave-current interactions and in predicting hurricane swells.

2.1.4 WW3 v. 2.22 comparison with other wave models in the Western Mediterranean (Ardhuin et al., 2007)

This study focused on defining the accuracy and identifying biases of wave forecasting models in the western Mediterranean. Wind forecasts are usually not as accurate in the Mediterranean as in the open oceans (Cavaleri and Bertotti, 2003, 2004). Many studies have highlighted the fact that winds in the Mediterranean are usually underestimated by coarse global models. The modeling periods chosen, 1st–31st October 2002 and 28th January–1 March 2003, were characterized by both mild wind conditions and severe storms.

Three wave models were evaluated, WAM cycle 4, WW3 version 2.22, and VAG, an operational model running at Météo-France that is based on a ''second-generation'' parameterization of the wave–wave interactions, with wind generation and dissipation formulations equivalent to the WAM cycle 4 model. Each was run with a directional resolution of 15 degrees. The WAM4 and WW3 grid frequencies were the same, beginning at 0.05 Hz and employing 30 frequencies logarithmically spaced with relative intervals of 0.1 from one frequency to the next. All systems were spun up for 24 hours, from 00 UTC on the 1st October and 28th January, and ran for about one month, until 00 UTC on 1st November 2002 and 1st March 2003, respectively. The model data domain covered the area from 30°N to 46°N and from 6°W to 36°30′E. The models were forced with wind fields from four sources: ALADIN (Météo-France model, ALADIN Int. Team 1997), with 10 km horizontal resolution wind fields at 3 hr intervals, the Coupled Ocean Atmosphere Mesoscale Prediction System (COAMPS) (operational Fleet Numerical Meteorology and Oceanography Center (FNMOC) model), with hourly wind forcing and a 27 km resolution, ARPEGE (global Météo-France model, Courtier et al., 1991) with 3 hrly wind forcing and a horizontal resolution of ~ 25km for the Western Mediterranean Sea, and finally the European Centre for Medium-Range Weather Forecasts (ECMWF) model, with a horizontal resolution of 40 km and wind fields produced every 6 hrs.

In situ observations came from several buoys in Italy, France, and Spain and one oceanographic tower in Italy. Most buoys were moored in coastal areas.

Besides in situ data, altimeter derived wave heights and wind speeds from ERS-2 and Jason were used. SeaWinds wind measurements from the QuikSCAT satellite, operated by NASA, were also used. These scatterometer winds were gridded at a 25 km resolution along the 1800 km wide swath of the satellite, with two passes per day.

Comparing the performance of the three wave models, it can be seen that the two third-generation models, WAM4 and WW3, behaved similarly for low wave heights. WW3 underestimated large wave heights in the Mediterranean Sea when ALADIN or COAMPS were used as meteorological input. The significant wave height (SWH or H_s) errors due to winds were comparable to those introduced by the wave model. However, for growing H_s there was a progressively increasing underestimation by WW3 compared to WAM. Scatter indices of H_s were identical for WAM and WW3 at open ocean buoys during October 2002, at 0.30, and best fit slopes were 0.92 and 0.87, respectively. At coastal buoys, WW3 had a scatter index of 0.43 vs. 0.48 for WAM.

A more definitive discrepancy was seen in comparisons with altimeter data. WW3 seemed to underestimate substantially the largest wave heights in the Mediterranean Sea. There was a clear tendency for WW3 to increasingly underestimate higher Hs values. This was confirmed by a similar comparison with buoy data. When compared to Jason and ERS-2 data, WW3 had a lower SI (0.21) than WAM (0.25) as well as a lower best-fit slope (WW3 = 0.86 vs WAM = 0.95) for the February simulation. Actually, the maximum H_s value reported during the test periods was about 12, 9, and 14 m for WAM, WW3 and VAG, respectively. There was also a general tendency toward underestimating the peaks with WW3. This behavior was associated with stormy events. In the low-value range, however, the statistics of WW3 were better, by a few percentage points, than those of WAM. In this range Bidlot et al. (2002) reported a tendency of WAM to overestimate the low wave heights, but the overall performance suggests, on average, values too low with WW3. Given acceptable performance of WW3 in the open oceans (see Tolman, 2002a; and Rogers et al., 2005), the present negative bias seems to be attributed more to the limited dimensions of the Mediterranean Sea. Most likely it can be corrected by retuning the model parameters.[3]

2.1.5 Comparison of five wave models around Australia (WW3 v. 1.15; Woodcock and Greenslade, 2007)

The operational consensus forecast (OCF) scheme (Woodcock and Engel 2005, referred to as WE05) uses past simulations to bias correct and combine model forecasts in order to produce a more accurate forecast in areas where observations are available. Each real-time OCF forecast consists of a weighted average of the set of latest-available, bias-corrected, component

[3] Again, this is consistent with our experience, that TC96 may require different calibration at different scales. However, we did not notice any problems with the default TC96 tuning applied in the Gulf of Mexico, which is similar in size to the Mediterranean. A possible explanation: the Gulf of Mexico is much more "open" than most areas of the Mediterranean, so it can be reasoned that the latter has characteristics of an open basin much smaller than the former.

forecasts, and every component projection is weighted by the inverse of the mean absolute error (MAE) of that forecast over the evaluation period. In this study, OCF used past observations and forecasts of SWH from five numerical wave models and at 18 wave observation locations around Australia to generate 24 hr predictions of significant wave height. The main objective was to investigate whether OCF improved on its component forecasts.

Observational data and model forecasts used in this evaluation began on 1 November 2003 for Waverider shallow buoys (in a depth of less than 25 m) and began on 16 July 2004 for Waverider deep-water buoys. The evaluation period ended 31 May 2005. The Australian wave data network observations were used to bias correct, weight, and verify the forecasts. There were five shallow-water buoys and 13 deepwater buoys.

The first three models used in this study were variations of AUSWAM, a version of the third generation WAM (WAMDI Group 1988; Komen et al. 1994). All three AUSWAM models (Greenslade 2001) were set up with different sources of wind forcing, domain sizes, and spatial resolutions. WAMMES (regional Australian domain, 1/8 ° resolution, 1 hourly wind forcing), was a deep water model nested within WAMAUS, which is another deep water model with regional domain, 1/2 ° resolution, 1 hourly wind forcing, and data assimilation. WAMAUS was, in turn, nested within WAMGLOB, characterized by a global domain, 1° resolution, 3 hourly wind forcing, available (again, fairly limited) shallow water physics options, and no data assimilation. The fourth model was the British Met Office (UKMO) second-generation wave model, with a global domain, 5/6° x 5/9° resolution, 1 hourly wind forcing, and available shallow water physics that also included the assimilation of altimeter wave heights (Holt 1997). The fifth model was WW3, here with a global domain, 5/4° x 1° spatial resolution, 3 hourly wind forcing, no data assimilation, and available shallow water physics included for regional runs. The global WW3 functions only to a minimum depth of 25 m, so shallow-water predictions of SWH derived from WW3 were unavailable. The differing configurations of the five models generated errors that varied between the models, thereby improving the probability of enhanced forecasting from an agreement of bias corrected model forecasts. The success of compositing techniques partially depended on the extent to which these errors were random and out of phase.

The 24 hr model forecasts of SWH were generated at the Waverider buoy sites every 12 h by cubic spline interpolation from the nearest model grid points to the buoy location. Significant wave height observations were averages in time at individual locations while the model forecasts were expected values of SWH over the model grid domain and time step. All SWH estimates used in the study, including the various model forecasts, signified different spatial and temporal scales.

The results were calculated based on 4,239 independent forecasts over 13 deep-water sites for the 29-event validation period. WW3 significantly (more than a 95% level based on RMSE) outperformed all of the other models. It yielded the lowest RMSE (0.53 m), mean absolute error (0.36 m), maximum absolute error (2.77 m), and scatter index (SI=27%), as well as the largest percent variance (V=70%). However, each raw forecast scheme bested the others in at least one buoy location. WW3 results improved even more from linear regression correction than from bias correction, continuing to outperform the other models. The linear regression increased the performance gap between WW3 and the other models, so compositing was less beneficial than

bias correction. Actually, neither performance-weighted nor equal-weighted composites were an improvement over the linear regression-corrected WW3.

The best model in shallow water was the highest resolution model, WAMMES, but this was due to its smaller bias. Once bias was removed, the models performed similarly, capturing about 50% of the daily variation in SWH. In deep water, the models achieved far better than persistence. The best forecasts came from a "composite of composites", where models with highly correlated errors were combined before being included in the performance-weighted, bias-corrected forecast. In deep water, a 20%–30% improvement in SWH over model forecasts was accomplished using the OCF strategy of performance-weighted compositing of bias corrected model forecasts. The OCF strategy (i.e., performance-weighted bias correction) yields approximately a 15% improvement on the raw WW3 forecasts. Bias correction alone improved WW3 by 13% so that compositing was not the dominant factor in forecast improvement.

2.1.6 Validation of a Multi-Grid WW3 Modeling System (WW3 v. 3.14; Chawla et al., 2009)

A validation study has been conducted recently by Chawla et al (2009) on the multi-grid WW3 system in a global domain using a mosaic of eight grids (http://polar.ncep.noaa.gov/mmab/papers/tn281/multi_hindanalysis.pdf). Results from that study revealed a seasonal bias in the Northern Hemisphere, positive biases (mostly in swells) in the central and eastern parts of the ocean basins and negative biases along the western margins. From spectral analysis, the wind wave portions of the spectra generally showed a negative bias. In the Southern Hemisphere a consistent, years-long positive bias has been observed, coinciding with an increase in the more energetic parts of the input wind field.

Table 2-1: Parameters of non-Navy WW3 validation studies.

Non-Navy Studies					
Author(s)	**Tolman 2002a**	**Tolman et al 2002**	**Tolman et al 2004**	**Ardhuin et al 2007**	**Woodcock & Greenslade 2007**
WW3 version, comparisons	WW3 v 1.15 with WAM	NOAA global WW3 with WAM	WW3 v 2.22 With NAH and WNA regional models	WWW v 2.22 with Western Med wave models: WAM cycle 4, VAG	OCF from 3 numerical wave models
Dates	Dec 1994 to Feb 1995	12 Jan 1998 - 30 June 1998	6 - 19 Sept 2003	1 - 31 Oct 2002, 28Jan–1Mar 2003	1 Nov 2003; 16 July 2004; 31 May 2005
Region	Global 78°N to 78° S	Global 78°N to 78° S	US east coast; Hurricane Isabel	W. Mediterranean 30°N to 46°N, 6°W to 36°30'E	Global, regional Aust. domains
Grid Resolution	1.25°×1°	1.25°×1°	Global: 1.25°×1° Regional: 0.25°	0.1°lat/lon	Variable between five models
Source wind forcing	GDAS	Wind, temp (GDAS, MRF), 3 hr intervals, T170 res with 42 levels	3 hourly analysis of GFS model (WNA) Hourly high res winds from GFDL model (NAH)	ALADIN – 10km horiz res - 3 hr int; COAMPS – 27 km res, hourly; ARPEGE - ~25km res, 3 hr interval; ECMWF – 40 km res, 6 hr interval	
Observations used: in situ	WMO buoys	NDBC buoys	NDBC buoys	Buoys, one oceanographic tower in Italy, France, Spain, mostly coastal	Shallow-water and deep-water Waverider buoys
Observations used: satellites	ERS-1	ERS-2	Jason-1	ERS-2, Jason NASA QuikSCAT	none
Skill	RMSE 15% of observed wave height	Overestimated wave heights by about 10%.	NAH - wave height bias at buoy = 0.01, RMSE of 0.68, and SI 23%. WNA bias-0.35, RMSE 0.80, and SI 27%.	At coastal buoys, WW3 had a scatter index of 0.43 vs. 0.48 for WAM. Open ocean was about the same.	Outperformed four other WAM-based models in deep water (>25 m)

2.2 Navy Validation Studies

2.2.1 WW3 vs. WAM – Implementation of WW3 at FNMOC (Wittmann 2001)

WW3 replaced WAM at FNMOC as its operational wave model in 2000. Compared to WAM, WW3 uses 40% less memory but about 30% more CPU time. This translates to about 320 MB of memory on the Cray C90 for the global implementation and 1260 CPU seconds/24 hour integration for WW3 vs. WAM's 560 MB and 960 CPU seconds/24 hour integration.

During January and February 2000, the models were run in parallel on a global 1° latitude by 1° longitude grid. WW3 was forced by the Navy Operational Global Atmospheric Prediction System (NOGAPS) 10-m winds, while WAM was forced by NOGAPS surface wind stress. The models were run on a 6-hourly update cycle using the forecast wave spectra as the initial condition for the next run. WW3 used bottom friction to dissipate wave energy where the bottom depth influenced the waves. WW3 and WAM both archived significant wave height, peak wave period, and wind speed.

The models were verified using 48 NDBC wave buoys and ERS-2 altimeter wave height measurements. Statistics such as mean bias, RMSE, and SI were computed after interpolating the significant wave height and peak wave period from the wave models to the wave measurement locations. Model nowcasts were interpolated to the ERS-2 data locations using a 6-hour time window centered on the 00, 06, 12, and 18 UTC synoptic times.

ERS-2 error statistics were based on measurements from ten regions: the North Pacific, equatorial Pacific, South Pacific, North Atlantic, US West Coast, Australia, South America, Equatorial Atlantic, South Atlantic and the Indian Ocean. When comparing the ERS-2 data, which had an order of magnitude more observations and much greater spatial coverage than the buoy observations, WW3 was favored over WAM in most metrics. For January 2000, WW3 had a slightly smaller RMS error (0.58 m) and scatter index (19%) than WAM (RMSE = 0.63 m; S.I. =22%), mainly due to better agreement in the 6 to 10 m wave heights. WAM showed a slightly larger bias in wave height (-0.22 m) than WW3 (-0.20 m).

When comparing the models with buoy observations for significant wave height, WAM's bias and RMSE were slightly smaller for the nowcast (-0.16 and 0.62 m, respectively) than WW3 (-0.26 and 0.67 m) but the correlation coefficients were identical for both models (0.92). WW3 better followed the wave height range, while WAM was comparatively unresponsive[4] and had a high bias. Both models underestimated the maximum periods (> 20 sec) at the start of swell events. Although WAM's RMSE was smaller in most areas, WW3's RMSE was smaller in the equatorial Pacific and the north Atlantic.

Validation with respect to the buoy data varied regionally and tended to favor WW3 over WAM in swell-dominated regions. However, the combined results from all of the buoy data showed no significant differences in skill between the two models. WW3 performed as well or better than WAM during the operational test period and ran more efficiently on FMNOC's higher memory platforms.

[4] See prior footnote.

The operational implementations of WAM at NAVOCEANO and WW3 at FNMOC are also discussed in Jensen et al. (2002).

2.2.2 Investigating Sources of Error in Low Frequency Energy Prediction in WAM4 and WW3 Models (Rogers, 2002)

This study sought to improve Navy surf and general global wave forecasts by identifying the causes of error in the WAM4 and WW3 models, with an emphasis on low frequency wave energy, of which swell is composed. Two wind forcing sources were compared: those from NOGAPS, and NCEP analyses produced by GDAS and the aviation cycle of the MRF model. NOGAPS is used by FNMOC and NAVOCEAMO to force the WW3 and WAM4 models. The model's coarse 1° resolution is thought to be adequate to represent the variability of the global wind forcing, which is dominated by large extra-tropical systems. Scatterometer data from the QuikSCAT satellite was used to derive snapshot wind fields to force the wave model.

Three categories of error sources included numerics and resolution, physics, and forcing. Errors in wind forcing with regard to the Navy's atmospheric model/wave model system were addressed for the first time in this study, using global wave model hindcasts with different wind forcing models. Issues such as low-frequency wave energy in oceanic-scale models are likely to have significant impact on modeled integrated parameters.

Winter wind field accuracy was hindcasted in the northeast Pacific Ocean in January 2001, when storm systems generate swells that are still young when they reach California buoys. A strong negative bias by NOGAPS of -1.20, (more so than NCEP at -0.71) was revealed at high wind speeds. A second hindcast for wind field accuracy was done in the southern Pacific during July 2001, when strong storms in this region also generate a great deal of low-frequency energy. NDBC buoys around the Hawaiian Islands and the western U.S. coastline measured these swells. NOGAPS again was biased low at high wind speeds (-0.14 and -0.15 for first order and ultimate quickest numerics, respectively).

Numerics and resolution were determined not to be dominant sources of low-frequency energy prediction error by Navy global wave models. The physics were also not a significant source of error, although it does play a role in low-frequency energy prediction. The dominant source of error appeared to be due to wind forcing inaccuracies, which was consistent with previous investigations. The operational implementation of NOGAPS that produces the surface wind fields used to force the global models tends to underpredict the strength of high wind speed events.

2.2.3 Quantifying the Role of Wind Field Accuracy in WAM4 and WW3 (Rogers and Wittmann 2002)

This report details the second part of a study to determine the role of wind field accuracy in the U.S. Navy's two operational, global scaled models of wind-generated surface waves, WAM4 and WW3. Three wind analysis sources were used in this comparison: NOGAPS, used by FNMOC and NAVO to force global wave models, NCEP analyses from GDAS and the MRF models that are used to force NCEP's WW3 model, and NOGAPS analyses with NOGAPS wind vectors replaced by QuikSCAT measurements when and where appropriate. This last method was used to better understand the impact on the wave model of the deviation of NOGAPS from measurements. All wave model results were run in hindcast mode. The NOGAPS and NCEP analyses were run with a three-hour interval on a twelve hour cycle. The blended QuikSCAT/NOGAPS analyses were created on a 3-hour time interval.

Relative impacts of the various sources of error were examined, including numerics/resolution, physical formulations at both the generation and propagation stages, and model sensitivity to wind field specification methods. Simulations during the winter seasons of January 2001 and January/February 2002 were made off the U.S. west coast to study physical formulations at the generation stage. A hindcast of July 2001 was made to study model skills at propagation stages. Wind forcing accuracy was determined by comparing NOGAPS and NCEP analyses to QuikSCAT measurements in the northeast Pacific during January 2001 and in the south Pacific during July 2001. Global comparisons were also made for the Jan 1 to Feb 8, 2002 time period. For those areas not within the NDBC U.S. and Canadian buoy networks, TOPEX and ERS-2 altimeter data were used.

Wave comparisons were made between operational FNMOC WW3 analyses vs. buoy data, operational FNMOC WW3 analyses vs. ERS-2 data, and WW3 hindcasts vs. buoy data, TOPEX data, and ERS-2 data for 8 January through 8 February 2002 time period. The degree of bias in the FNMOC buoy comparisons varied significantly by region.

Based on previous findings, the role of numerics/resolution on wave model error statistics was discounted as a first order source of error. With accurate wind forcing both WAM4 and WW3 reliably predicted low frequency energy and, to a greater degree, total energy. The models showed significant differences in wave growth in low frequency energy comparisons, but were very close in predictive skill at the generation stage. Attenuation seemed under predicted in the WAM4 model, consistent with previous observations, but these conclusions were tentative.

The direct cause of negative bias in total wave energy (wave height) was traced back to the Navy's operational surface wind product, most evident at higher wind speeds and varying considerably between seasons and regions. The negative bias in the NOGAPS surface wind analysis was attributed to the Emanuel cumulus parameterization within NOGAPS. The negative bias of WW3 compared to ERS-2 data was -1.24 on the West Coast (from 120°E to 290°E, 24°N to 68°N) and -2.38 in the North Atlantic, with a global mean bias of -1.02. The cloud scheme of Teixeira and Hogan (2002) improved surface bias wind in the tropics. Upgrades to the NOGAPS horizontal and vertical resolutions in September 2002 from T169L24

(80 km horizontal resolution, 24 vertical levels) to T239L30 (50 km horizontal resolution, 30 vertical levels) further reduced negative bias in the surface winds.

2.2.4 Evaluations of Global Wave Prediction at FNMOC (Rogers et al. 2005)

Rogers et al., (2005) examined only one test case in which significant improvement in the operational WW3 model hindcasts resulted from major improvements in operational surface wind forcing fields. While this is a predictable outcome, several other questions were considered:

- If two competing forcing fields are dissimilar in skill (as in comparing products from two operational centers, or comparing analysis fields versus forecast fields), does the more accurate field necessarily yield better wave model results?
- How might the metric for accuracy differ for a wave modeler than, for example, a circulation modeler?
- How important is random error relative to bias error?
- If a scenario can be identified where a wave model's representation of physics (generation, dissipation, and nonlinear interactions) is likely to be the primary source of error, is the wave model bias positive or negative? How does the answer depend on the frequency, i.e., the wave number range considered, or perhaps on the geographic location?

These questions were addressed using hindcasts specifically designed for this purpose. A review of the model errors is given.

Improvements in WW3 over WAM4 over time indicate that geographic and spectral resolutions are not a primary source of bias. Total significant error in WW3 global wave model predictions come from both external (wind forcing) and internal (wave model physics, numerics, resolution) forcing. This study focused on internal error, with the understanding that there are major challenges in apportioning external and internal error. Three tests (1a, 2a, 3a) were constructed to quantify bias associated with wave model source/sink terms, and two (Tests 2a and 3a) were applied and discussed in this study. The Test 2a hypothesis is that if a model is forced by a wind field with a bias of known sign, and nontrivial bias of opposite sign is observed in energy predictions from a wave model forced by this wind field, then a probable bias associated with the wave model itself must exist. Test 3a hypothesized that when hindcasts and wave model-data comparisons are chosen to minimize bias from numerics and resolution, then any significant bias in the wave model itself (i.e. internal bias) is likely associated with the model's source/sink term parameterizations.

The hindcasts in this study differ from those done in Rogers (2002) in that they are more recent, of longer duration, and are limited to the wintertime in the Northern Hemisphere. The two hindcast periods were from the winters of 2001/02 and 2002/03 (1 Dec to 3 March). During each winter season, the hindcasts were forced by both NOGAPS and a blended NOGAPS/QuikSCAT data. Using 1° geographic resolution, four hindcasts were set up and performed in comparable fashion to the global implementation of WW3 at FNMOC prior to 2002.

Seven NDBC buoy spectra were used as ground truth for the model validation. Observations from four buoys located in the northwest Atlantic were characterized by an even mixture of seas and young swells. There were three buoys moored in the northeast Pacific in an area dominated by swells.

The results of the validation studies showed that bias in the 2002/03 wind fields was not a primary cause of bias in the wave hindcast results and further improvements to the wind field bias would not necessarily lead to improvements in wave predictions. Furthermore, more accurate wind forcing did not lead to more accurate wave predictions. Comparisons of the results from the wind field validations (in Rogers et al. 2004) and wave validations in this study suggested that wind bias at both moderate and high wind speeds was much more critical than wind speed RMSE when determining wave prediction skill. The model hindcasts tended to significantly overpredict energy at higher frequencies and to underpredict energy at lower frequencies. For the winter of 2002/2003, WW3 hindcasts in the Atlantic (at the 0.04 Hz frequency) showed a larger negative bias (-0.32) with NOGAPS forcing than with NOGAPS/QuickSCAT forcing (-0.14) compared to buoy observations. This was true at all frequencies in the Atlantic. The simulations in the two oceans differed in the frequency at which their bias changed sign, at 0.06 Hz (-0.22) in the northeast Pacific and at 0.12 Hz or higher (0.04) in the northwest Atlantic. Negative bias was observed over most of the model's frequency range in the Atlantic. In the Pacific there was a higher positive bias with the NOGAPS/QuikSCAT forcing (0.24) at 0.04 Hz than with just NOGAPS forcing (0.20). Correlation coefficients and RMSEs were fairly comparable between the two modes of forcing. In the winter 2001/2002 study, stronger negative biases are seen in both the Atlantic and Pacific for all frequencies with the NOGAPS forcing. Due to the apparent error associated with the WW3 physics, the model and future operational nowcasts/forecasts should receive additional tuning, similar to that performed by Tolman (2002d), and possibly other enhancements to the physics.

2.2.5 WW3 Transition to Operations (Dykes and Rogers 2011)

This paper was presented at the University of New Orleans Ocean Waves Workshop (http://www.uno.edu/research/UNOResearch/OceanWaves), November 11 2011, and is reproduced in full in Appendix A.

Table 2-2: Parameters of Navy WW3 validation studies.

Navy Validation Studies				
	Wittmann 2001	**Rogers 2002**	**Rogers & Wittmann 2002**	**Rogers et al 2005**
WW3 version, comparisons	WW3 vs WAM at FNMOC	Error sources in low frequency energy pred WAM4 and WW3 models	Role of windfield accuracy in WAM4 and WW3	Evaluation of global wave prediction at FNMOC
Dates	Jan to Feb 2000	Jan 2001, July 2001	Jan 2001, July 2001, 1 Jan to 8 Feb 2002	1 Dec – 3 March 2001/02 and 2002/03
Region	Global, 7 regions	US east coast and N. California	NE and southern Pacific	Global, N. California comparisons
Grid resolution	1°×1°			
Source wind forcing	WW3: NOGAPS 10 m height winds; WAM: NOGAPS surface wind stress	NOGAPS, NCEP, NOGAPS w/QuikSCAT		
Observations used: buoys	NDBC wave buoys	NDBC buoys around Hawaiian Island and western US coastline	NDBC and Canadian buoys	NDBC buoys in N Atlantic, NE Pacific
Observations used: satellites	ERS-2 altimeter wave height measurements in 10 regions	QuikSCAT (for winds)	TOPEX and ERS-2 satellite altimeter data	QuikSCAT (for winds)
Skill	Global WW3 - lower RMSE and SI than WAM, Regional WW3 lower RMSE in most regions against ERS-2. Mixed results for buoys comparisons.	Analyses biased low at high wind speeds. Slight bias w/ NCEP, and significant in NOGAPS, esp. in NE Pac. Neg. bias over most of WW3 freq. range.	Error due more to model forcing than due to physical formulation	Neg. bias in total wave energy; strong surface wind events in the NOGAPS analyses were biased low.

3.0 REALTIME MULTI-GRID WAVEWATCH III®

Contributing authors: James Dykes and Kim Watson

Currently WAM is the operational model run at NAVOCEANO and WW3 is the model soon to replace WAM. The goal is for WW3 to perform comparably if not better than WAM within the same or lesser timeframe in producing accurate wave forecasts for primarily providing boundary conditions to small scale wave models covering at many locations in the world. Here performance is measured by timeliness in producing model results given certain resources and accuracy of the results as they compare to observational data. One type of observational data source—buoy data—is used here as ground truth to compare with model forecasts. Comparison to observations in this section serves as cursory verification of the model performance. For comprehensive validations, we refer the reader to Sections 2 and 4.

3.1 Domain Configuration

Grids include a global domain, the eastern Pacific, surrounding Central America, western Atlantic, Mediterranean Sea, the North Indian Ocean and the western Pacific. Domains considered additional are off the US west coast, surrounding South America, and surrounding Australia. Because this is a multi-grid system, all domains are run concurrently as a single modelling system. Figure 1 provides a view of the model domains in the WW3 multi-grid system for these runs.

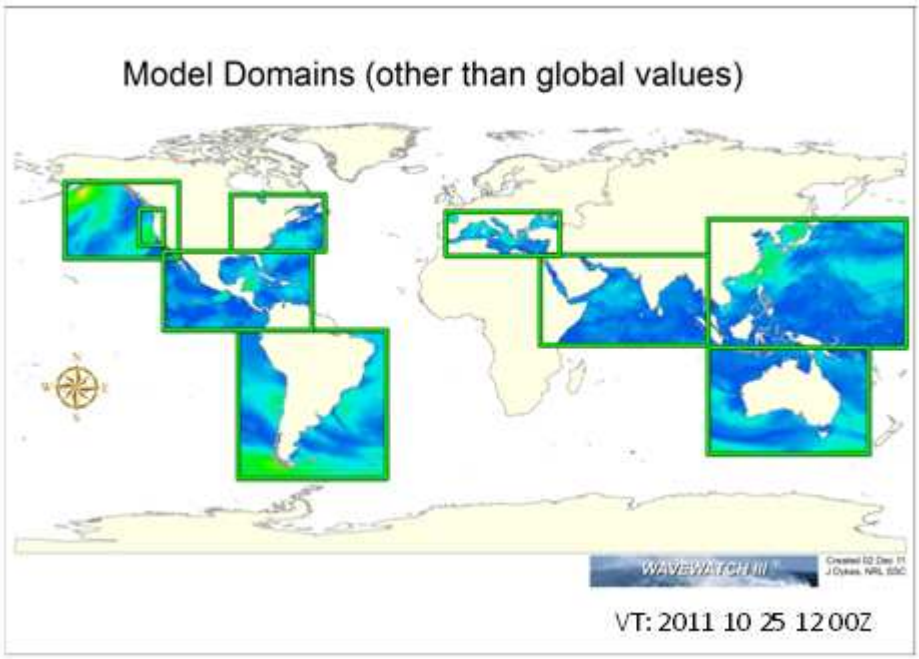

Figure 3-1: Multi-grid domain of ten regions (includes the global domain) running concurrently at NAVOCEANO.

Both WW3 and WAM have been running at NAVOCEANO on 12-hour cycles beginning at 00 and 12 UST. The output results are in the form of netCDF files formatted using the NAVOCEANO-augmented Cooperative Ocean/Atmosphere Research Data Service (COARDS) conventions, which facilitated the processing of the model output for analysis and comparison to other data. The model setup is fixed. Tolman and Chalikov (T&C, or "ST2") physics (Tolman and Chalikov, 1996) are used here. The model version used is v4 (a development code), though in this section, we only use features that were already available in v3.14.

The ten domains have been running in the quasi-operational mode since January 2011. Table 3-1 provides a list of domains accompanied by their grid spacing and domain extents. Some variations to the original similarly named WAM domains at NAVOCEANO are that the *eur_n2*, *n_ind_n2* and *w_pac_n2* domains were made smaller to minimize overlap with each other. Also, some of these domains WW3 are higher resolution, i.e. smaller grid spacing, than for WAM. All domains use a computational grid that is rectilinear in the latitude-longitude coordinate system.

Table 3-1: Realtime model grid domains. WW3 grids with COAMPS forcing are given in **bold.**

Domain Name	Area	Grid spacing	West	East	South	North
Global05	Global	0.5	0.0	360.0	-77.0	77.0
e_pac_n2	**E. Pacific**	0.2	-160.0	-114.0	29.0	60.0
us_wcoast	**US West Coast**	0.1	-130.0	-120.0	34.5	49.0
centam_n2	**Central America**	0.1	-120.0	-60.0	0.0	32.0
w_atl_n2	**Western Atlantic**	0.1	-93.0	-55.0	32.0	55.0
eur_n2	**Europe**	0.1	-6.0	40.0	30.2	47.9
n_ind_n2	**N. Indian Ocean**	0.2	32.0	100.0	-6.0	30.6
w_pac_n2	**W. Pacific**	0.2	100.0	180.0	-7.0	45.0
s_america	S. America	0.2	-90.0	-30.0	-60.0	0.0
aus_n1	Australia	0.2	100.0	165.0	-50.0	-7.0

Note: The *Global05* computational domain actually extends from -90 to 90 but is effective to the extent as listed above, because the areas near the poles are not specified as sea points.

Historically, WAM regional nests at NAVOCEANO and WW3 regional nests at FNMOC (both using one-way nesting) were configured to coincide with regional atmospheric models (i.e. COAMPS domains). The key feature of this domain design is that it distinguishes it from comparable configurations at NCEP, which puts more emphasis on the global atmospheric product, GFS. The former approach has been taken in the multi-grid design here. WW3 domains with COAMPS forcing are given in **bold** in Table 3-1. Notice that not every regional domain corresponds to a COAMPS domain. The additional domains surrounding South America and Australia represent high resolution wave model computation with relatively coarse (global) wind

forcing, similar to NCEP regional domains. Similarly, the US West Coast domain does not have its own COAMPS counterpart, but is driven with the same winds as the eastern Pacific domain.[5]

The coverage is almost completely mutually exclusive, that is coarse domains do not need to cover fine resolution or small grid spacing domains, organizing then into a tier level system as prescribed by the multi-model system. Therefore, the global domain, *Global05*, only runs with computational points set primarily outside of the other domains, which are arranged at a lower tier. Among the lower tiered nests, only two domains appear to have any overlap, *centam_n2* and *e_pac_n2*, with the former yielding to the computations of the latter.

All the domains in the WW3 test case use spectral components consisting of 25 distinct frequencies at 36 directions with a 5-degree offset, i.e. starting at 5 degrees from north. Starting frequency is 0.04118 and the increment factor is 1.1. We use a fairly large time step for the global domain, with 3600 seconds as maximum global time step. For all the other domains, the same time step is 360 seconds. For the CFL time step, we use 1800 seconds for the global grid and up to 360 seconds for the other grids.

For each of the domains, bathymetry with 2-minute resolution was extracted from the DBDB2 global topography database developed at NRL (Ko, 2002) and interpolated to the grid spacing of each of the domains. Although the model can accept ocean surface currents and water levels, neither is input at this time. For the global domain, a stationary ice field is used that roughly represents the average coverage throughout the year. (In the transitioned system, this should be replaced with a non-stationary field. This is discussed further below.)

3.2 Results of WW3 and WAM Comparisons to Buoy Observations

To give an idea as to the performance of WW3 compared to the current operational system, the following results show the comparison of the models to observations for significant wave height. Selected buoys, located within domains provided by both WAM and WW3, were chosen for the validation and are labeled accordingly in the figures. The name of the WW3 domains is used whilst the name of the equivalent WAM domain is similar enough to be understood, e.g. w_atl_n2 for WW3 corresponds to w_atl_nest2_appl for WAM. A software routine was used to interpolate the values from the model grid at points coinciding with buoy locations.

A sample of scatter plots are included in the figures below and tables provide summary statistics for the model comparisons to selected NDBC buoys located in waters around the United States. The 00- and 24-hour forecasts were compared to the observations. Statistics include mean bias (MB), root mean square difference (RMSD, used interchangeably with RMSE), slope, correlation coefficient (CC), and scatter index (SI) for both models. SI has been considered well–accepted and useful metric according to much of the literature. For each month the number of samples ranges from 55 to 62 depending on the month. Mostly the locations in shallow water or near coasts are addressed here, because our primary interest is the output that will be used as boundary conditions for coastal wave models.

[5] At time of writing, we can confirm the following COAMPS regions presently running at FNMOC: 1) Central America, 2) Eastern Pacific, 3) Europe, 4) Hawaii (2 grids), 5) Northern Indian Ocean, 6) Southwest Asia, 7) Western Atlantic, and 8) Western Pacific.

Comparisons in total represent up to five month time periods. Figures 3-2 and 3-3 show scatter plots, and Table 3-2 lists statistics, for model output for western Bermuda compared to NDBC buoy 41048, located at 31.978 N and 69.497 W for January through April 2011. Figures 3-4 and 3-5 show scatter plots, and Table 3-3 lists statistics, for model output for Tampa Bay compared to NDBC buoy 42036 located at 28.500 N and 84.517 W for January through March and July 2011, with a depth of 54 meters. And Figures 3-6 and 3-7 show scatter plots, and Table 3-4 lists statistics, for model output for waters off the US west coast compared to NDBC buoys 46028 located at 35.7 N and 121.88 W and 46006 located at 40.84 N and 137.49 W for April through August 2011 and 46002 located at 42.52 N and 130.32 W for June through August 2011.

Readers who have access from within the .navy.mil domain can see addition plots at https://www7320/Alvin/index.php/WW3_Validation_Test_Report, each corresponding to values shown in Tables 3-2, 3-3, and 3-4 (only highlighted values have corresponding plots here). This wiki also includes comparisons between altimeter data and a multi-grid hindcast run on NAVOCEANO machines. Since this section deals with the real-time system, those results are not reproduced here.

For the comparison to NDBC buoy 41048 (240 NM west of Bermuda in the western North Atlantic), the most pronounced difference seen is that the mean bias for WW3 is always smaller than WAM, i.e. both wave model forecasts are low, but WAM is consistently lower. The RMSD values for WW3 are lower than WAM comparable. WW3 has always significantly higher slope of the regression line for the scatter. Correlation coefficients are comparable, WAM more often a little higher. Scatter index is consistently slightly lower for WW3 than for WAM.

As far as the comparisons to NDBC buoy 42036 outside Tampa Bay (located in the Gulf of Mexico), all but one of the statistics between the models is comparable with neither having a clear advantage. The slope is consistently and significantly higher for WAVEATCH III.

For NDBC buoy 46028 located off the US west coast near Morro Bay, the statistical comparisons are more extreme, probably due to the diversity of wave conditions that would be expected when exposed to the vast Pacific area. Mean biases for WW3 whether they were positive or negative were most times still less than that for WAM. The RMSD for WW3 is significantly lower than WAM for all but one month. The slope and CC are comparable between the two models except in July, WAM was particularly unskillful. Scatter index is consistently lower for WW3 than for WAM.

So far, model values at locations close to the coast or in relatively shallow water were compared to observations showing modest results. We go on to show two other locations the deep water at 46006 and 46002 in the eastern Pacific domain with results in Table 3-4. Here it is clear that the skill of both models improves overall. But, WW3 improves more significantly than WAM. At this point the 24-hour forecast results are not included, because it is clear that the forecast skill changes from 00-hour to 24 are dominated by the skill of the model providing the wind forcing. This does not play out quite the same way on the Atlantic side although both models perform a little better away further away from the coast. That better case was already displayed in Table 3-2. Results of the comparisons of additional buoys are tabulated in Appendix C.

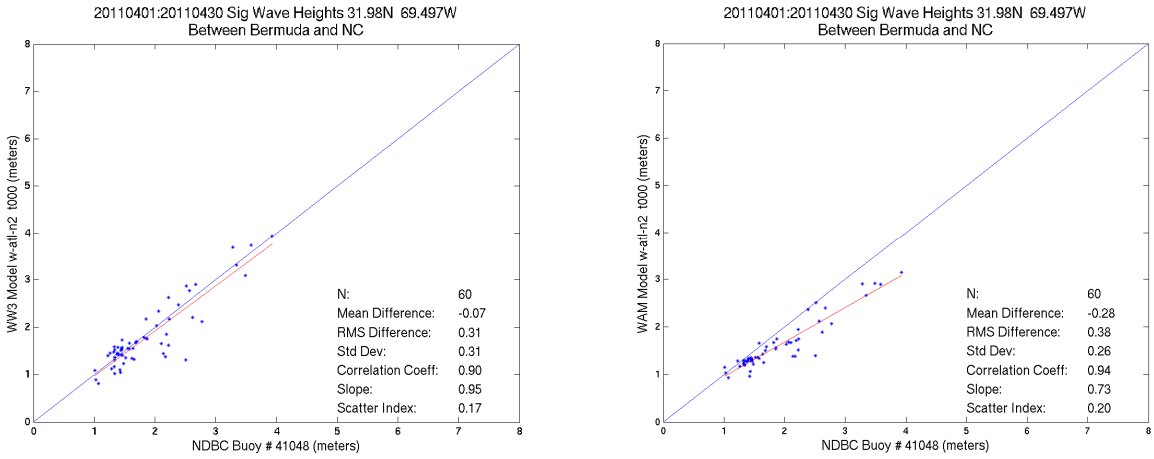

Figure 3-2: Scatter plots of SWH for WW3 (left) and WAM (right) in the model domains *w_atl_n2* and *w_atl_nest2_appl*, respectively, for 00-hr April 2011 forecasts compared to NDBC buoy 41048 observations located 240 NM west of Bermuda. Statistics are provided within the graphic as well as in Table 3-2.

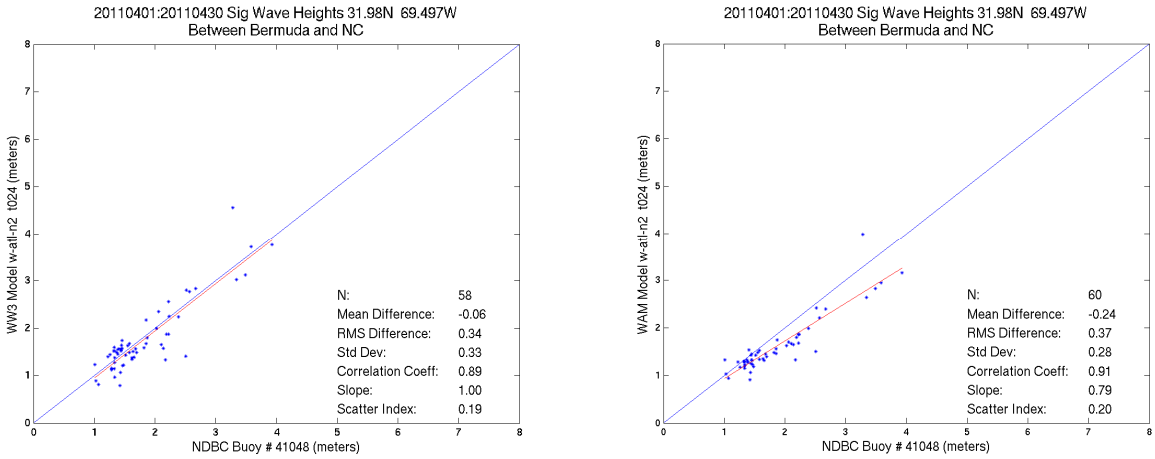

Figure 3-3: Scatter plots of SWH for WW3 (left) and WAM (right) in the model domains *w_atl_n2* and *w_atl_nest2_appl*, respectively, for 24-hr April 2011 forecasts compared to NDBC buoy 41048 observations located 240 NM west of Bermuda. Statistics are provided within the graphic as well as in Table 3-2.

Table 3-2: Summary statistics for WW3 and WAM output within domains *w_atl_n2* and *w_atl_nest2_appl*, respectively, compared to NDBC buoy 41048. Highlighted rows depict those shown in Figures 3-2 and 3-3.

240 NM West of Bermuda (NDBC 41048)										
Month/ Fcst Hr	**MB [WW3]**	**MB [WAM]**	**RMSD [WW3]**	**RMSD [WAM]**	**CC [WW3]**	**CC [WAM]**	**Slope [WW3]**	**Slope [WAM]**	**SI [WW3]**	**SI [WAM]**
Jan/00	-0.28	-0.36	0.49	0.53	0.94	0.96	0.97	0.72	0.20	0.22
Feb/00	-0.18	-0.32	0.39	0.42	0.95	0.97	1.00	0.83	0.17	0.19
Mar/00	-0.18	-0.30	0.36	0.42	0.92	0.93	1.02	0.72	0.17	0.19
Apr/00	-0.07	-0.28	0.31	0.38	0.90	0.94	0.95	0.73	0.17	0.20
Jan/24	-0.27	-0.36	0.49	0.52	0.93	0.95	0.93	0.74	0.20	0.21
Feb/24	-0.15	-0.30	0.43	0.40	0.93	0.96	1.06	0.90	0.19	0.18
Mar/24	-0.18	-0.31	0.37	0.41	0.92	0.93	1.07	0.75	0.17	0.19
Apr/24	-0.05	-0.24	0.34	0.37	0.89	0.91	0.99	0.79	0.19	0.20

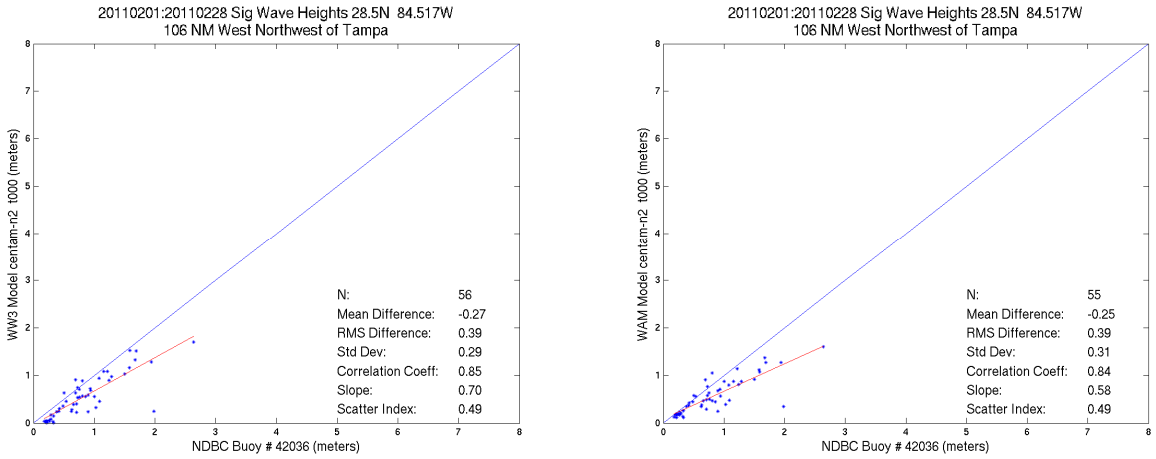

Figure 3-4: Scatter plots of SWH for WW3 (left) and WAM (right) in the model domains *centam_n2* and *cent_am_nest2_appl*, respectively, for 00-hr February 2011 forecasts compared to NDBC buoy 42036 observations located 106 NM west northwest of Tampa. Statistics are provided within the graphic as well as in Table 3-3.

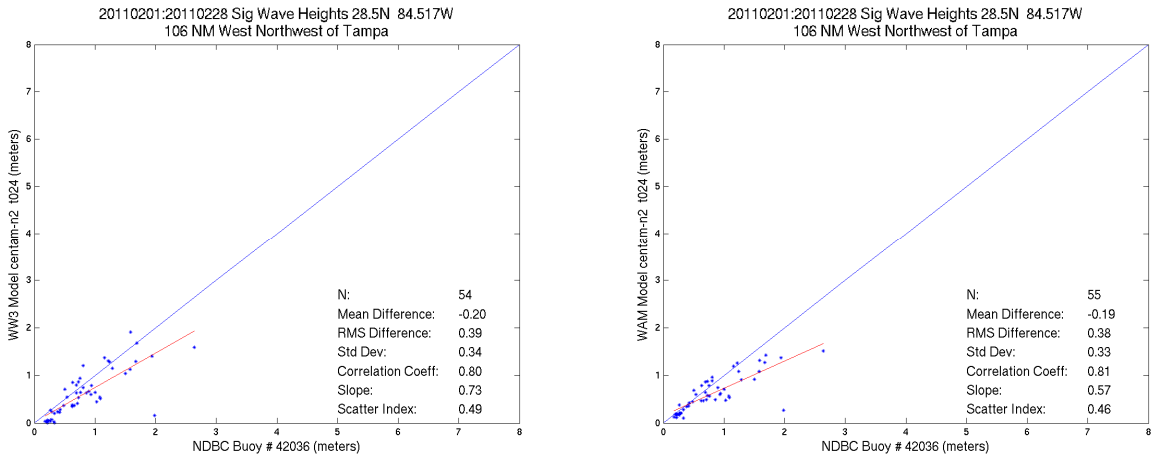

Figure 3-5: Scatter plots of SWH for WW3 (left) and WAM (right) in the model domains *centam_n2* and *cent_am_nest2_appl*, respectively, for 24-hr February 2011 forecasts compared to NDBC buoy 42036 observations located 106 NM west northwest of Tampa. Statistics are provided within the graphic as well as in Table 3-3.

Table 3-3: Summary statistics for WW3 and WAM output within domains *centam_n2* and *cent_am_nest2_appl*, respectively, compared to NDBC buoy 42036. Highlighted rows depict those shown in Figures 3-4 and 3-5.

106 NM West Northwest of Tampa (NDBC 42036)										
Month/ Fcst Hr	**MB [WW3]**	**MB [WAM]**	**RMSD [WW3]**	**RMSD [WAM]**	**CC [WW3]**	**CC [WAM]**	**Slope [WW3]**	**Slope [WAM]**	**SI [WW3]**	**SI [WAM]**
Jan/00	-0.29	-0.29	0.44	0.45	0.85	0.84	0.70	0.61	0.39	0.40
Feb/00	-0.27	-0.25	0.39	0.39	0.85	0.84	0.70	0.58	0.49	0.49
Mar/00	-0.20	-0.22	0.28	0.29	0.92	0.93	0.93	0.75	0.35	0.36
Jul/00	-0.19	-0.12	0.29	0.20	0.80	0.81	1.06	0.75	0.56	0.39
Jan/24	-0.25	-0.27	0.42	0.43	0.84	0.84	0.73	0.64	0.38	0.38
Feb/24	-0.19	-0.19	0.39	0.38	0.79	0.81	0.72	0.57	0.49	0.46
Mar/24	-0.13	-0.15	0.26	0.24	0.91	0.92	1.02	0.84	0.33	0.30
Jul/24	-0.15	-0.09	0.30	0.22	0.79	0.77	1.20	0.86	0.59	0.43

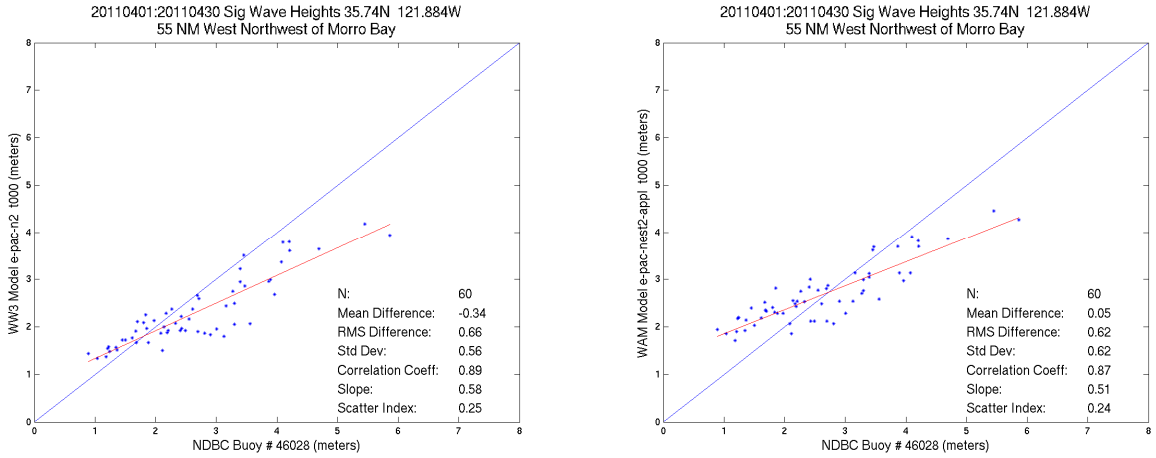

Figure 3-6: Scatter plots of SWH for WW3 (left) and WAM (right) in the model domains *e_pac_n2* and *e_pac_nest2_appl*, respectively, for 00-hr April 2011 forecasts compared to NDBC buoy 46028 observations located 55 NM west northwest of Morro Bay. Statistics are provided within the graphic as well as in Table 3-4.

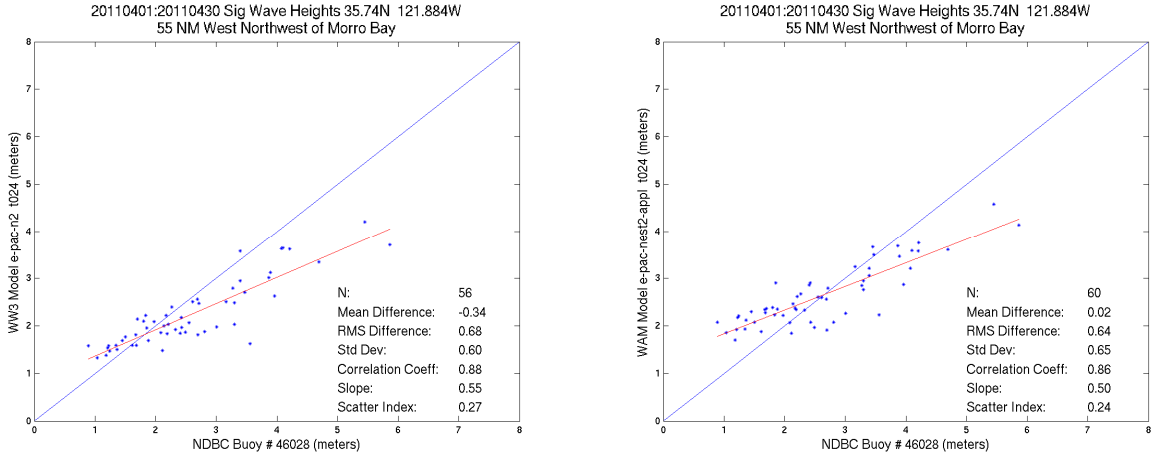

Figure 3-7: Scatter plots of SWH for WW3 (left) and WAM (right) in the model domains *e_pac_n2* and *e_pac_nest2_appl*, respectively, for 24-hr April 2011 forecasts compared to NDBC buoy 46028 observations located 55 NM west northwest of Morro Bay. Statistics are provided within the graphic as well as in Table 3-4.

Table 3-4: Summary statistics for WW3 and WAM output within domains *e_pac_n2* and *e_pac_nest2_appl*, respectively, compared to NDBC buoys 46028, 46006, and 46002. Highlighted rows depict those shown in Figures 3-6 and 3-7.

Month/ Fcst Hr	MB [WW3]	MB [WAM]	RMSD [WW3]	RMSD [WAM]	CC [WW3]	CC [WAM]	Slope [WW3]	Slope [WAM]	SI [WW3]	SI [WAM]
55 NM West Northwest of Morro Bay (NDBC 46028)										
Apr/00	-0.34	+0.05	0.66	0.62	0.89	0.87	0.58	0.51	0.25	0.24
May/00	-0.17	+0.32	0.44	0.53	0.74	0.73	0.62	0.71	0.19	0.23
Jun/00	+0.05	+0.46	0.34	0.59	0.81	0.77	0.69	0.62	0.16	0.28
Jul/00	+0.38	+0.64	0.57	0.89	0.59	0.13	0.49	0.11	0.31	0.49
Aug/00	+0.21	+0.66	0.36	0.71	0.76	0.84	0.51	0.57	0.21	0.41
Apr/24	-0.34	+0.02	0.68	0.64	0.88	0.86	0.55	0.50	0.27	0.24
May/24	-0.16	+0.30	0.46	0.55	0.71	0.71	0.64	0.73	0.20	0.23
Jun/24	+0.06	+0.44	0.36	0.59	0.79	0.73	0.66	0.56	0.17	0.28
Jul/24	+0.41	+0.64	0.60	0.91	0.55	0.08	0.45	0.07	0.33	0.51
Aug/24	+0.15	+0.59	0.36	0.67	0.64	0.69	0.43	0.46	0.21	0.38
600 NM West of Eureka, California (NDBC 46006)										
Apr/00	+0.27	+0.05	0.46	0.49	0.91	0.88	0.87	0.53	0.17	0.18
May/00	+0.05	+0.03	0.33	0.41	0.92	0.86	0.88	0.53	0.14	0.18
Jun/00	+0.22	+0.53	0.29	0.58	0.88	0.80	0.80	0.66	0.19	0.38
Jul/00	+0.10	+0.45	0.24	0.53	0.89	0.76	0.87	0.60	0.15	0.33
Aug/00	+0.13	+0.51	0.25	0.58	0.88	0.84	0.72	0.45	0.18	0.42
275 NM West of Coos Bay, Oregon (NDBC 46002)										
Jun/00	+0.17	+0.47	0.26	0.57	0.91	0.72	0.89	0.61	0.15	0.35
Jul/00	+0.16	+0.48	0.28	0.54	0.81	0.70	0.91	0.67	0.17	0.33
Aug/00	+0.12	+0.59	0.23	0.64	0.81	0.63	0.65	0.33	0.18	0.48

3.3 Technical Aspects

A full description the operational implementation of the modeling system including the operational environment being transitioned to NAVOCEANO is described on the NRL wiki, https://www7320.nrlssc.navy.mil/Alvin/index.php?title=WW3_Automated_Implementation, and will be published in an NRL technical memo report. Highlights of the operational model are described below. Basically, the cron starts a set-up script that checks for run eligibility and pre-processing conditions. When all the conditions are met and pre-processing is complete, a job is submitted into the Portable Batch System (PBS) to run the main modeling system. When that is complete, a post-processing script is submitted into PBS and the results are produced for consumption by users and other systems. While the main model run contains all the domains together at once, the pre- and post-processing steps are individually domain specific.

Changes to the transitioned system should rarely need any changes. Most of the user interaction will be the addition of spectra points to the list to satisfy requirements for boundary conditions for additional and on-going SWAN model domains. The addition of these points will be handled in ROAMER (Rapid Ocean Analysis Modeling Evaluation Relocatable, see Allard et al. 2002).

3.3.1 Model inputs

The model setup to be transitioned to NAVOCEANO requires bathymetry and winds and, for the global domain, ice. Also, a restart file from the last model run cycle is used or a cold start is generated if no restart is available. These inputs are pre-processed in a separate step during the setting up stage before the model run is prepared and submitted.

Generally, a global set of fields of wind and ice provided by the NOGAPS system are applied to the global model, and winds for regional domains are provided by the higher resolution COAMPS for their respective wave model domains. There are some exceptions where a regional domain would use the NOGAPS winds, generally when COAMPS winds are unavailable.

The original WAM system does not include ice in any manner. As mentioned above, in the implemented WW3 system, a stationary ice field is used that roughly represents the average coverage throughout the year. This can be considered as a placeholder. For the permanent system, it will be straightforward to replace this with a similarly formatted field that is updated routinely. According to files available in NRL archives, we observe that since March 2011, the NOGAPS output fields have included ice concentration values; presumably, these are derived from an ice model or radiometer analysis. So, these files are one option. In building the files for WW3, we recommend to double-check that ice concentration is read in correctly by outputting one ice field from WW3 and plotting (specifying concentration as a fraction where the model expects a percentage, or vice versa, is a common mistake).

The real-time system, as it has been running before its transition to NAVOCEANO, uses winds up to 48 hours, because the total system is set up to run to the shortest period of forecasts available from COAMPS as provided by operations at NAVO. The resulting forecasts, which thus far have been produced up to 48 hours, are the basis for the validation of the model. Further work will include an automated scheme that will extend the forecast period to 96 hours using the NOGAPS winds for those domains whose winds are not available that far into the forecast.

3.3.2 Recommended spin-up time

Since the transitioned system would rarely be changed, it is very unlikely that the system will have to start again when spin-up time has to be considered. After any interruption of the system, existing restart files can be used to resume run cycles. If by some small chance a domain has to be eliminated from the system or catastrophic failure occurs (e.g. nuclear holocaust takes out a file system), then the entire system would have to be restarted cold and run for a one week period before using the results.

3.3.3 Model output

During the post-processing phase, the output files that are in a format native to the model are converted into ASCII text and netCDF. Theses output include the bulk parameter fields and the point spectra. Restart files are also generated for the nest run cycle normally in 12 hours. The bulk

parameters include: significant wave height, mean wave period, mean wave direction, peak wave frequency, peak wave direction, wind sea peak frequency, and wind sea peak direction.

3.3.4 Resource requirements

In the pre-processing step, the work is done interactively in the cron and requires very few resources. In the post-processing step one processor is used and draws a modest amount of resources as well. The bulk of the processing time and memory space goes into the main run. The currently transitioned system on the IBM Power 6 IBM using an AIX OS uses 512 processors, 32 on 16 nodes using between 210 and 230 CPU hours. The wall-time for the 48-hour forecast has been 28 minutes, consistently. Most of the software needed for the system administration comes normally with a DoD Supercomputing Resource Center (DSRC) High Performance Computing (HPC) implementation. The exception is a set of Perl modules needed to support the automated system itself and the netCDF generation script.

3.3.5 Boundary conditions for outside nests

The current modeling system provides boundary conditions (BCs) consisting of spectra at water points surrounding candidate nests. During Talisman Sabre 11, a U.S. Navy bilateral exercise conducted May – July 2011 to train Australian and U.S. Forces in planning and conducting Combined Task Force operations, spectra were provided for a Simulating Waves Nearshore (SWAN) model domain off the coast of Australia. The procedure to process these points for use by an outside requirement posed no significant strain on the system.

3.3.6 Turn-around time

As this system is set up now to run on the HPC computer, DaVinci, on the DSRC with all ten domains in place as described above for a 48-hour forecast from start in the PBS to finish, the system wall clock time averaged about 28 minutes. This does not include the post processing as this could vary to a great degree depending on the connectivity of the archive machine, in this case, Newton. 512 processors were used and the model has been shown to scale very well on this architecture. Post-processing is done in a separate submission to PBS not attached to the main run. Otherwise, though using only one processor, the post-processing would cost the user the full 512 processor time.

3.3 Future Work

Increased efficiencies may be obtained depending on adjustments of optimizations related to the compiler, operating system and architecture, and on the model domain configuration. A new operational machine will soon replace DaVinci, so those optimizations are yet to be discovered. So, our focus can now point towards how the domains are set up, whether we can mask out large areas of insignificant change, and how to provide for obstructions smaller than the resolution of any of the domains.

4.0 VALIDATION OF GLOBAL (SINGLE GRID) HINDCAST

Contributing authors: Erick Rogers, David Wang, Kim Watson

4.1 Purpose

In this section we describe a validation of global model hindcast implementation. Two source term packages were compared, ST2 (which refers to the Tolman and Chalikov (1996) or "T&C" physics) and ST4 (which refers to the Ardhuin et al. (2010) "Test 441" physics). We look at swell dissipation and whether swell is overpredicted with T&C physics, as has been previously reported, and/or if it is corrected with Ardhuin et al. (2010) physics (Test 441). To help quantify the role of wind field accuracy in the global model hindcast, we also compared hindcasts from two different wind forcing fields. With two physics packages for each wind forcing field, a total of four hindcasts were generated. Wind forcing was also evaluated using bias-corrected altimeter data. The source of all wind and wave altimeter data in this study was Ifremer (http://www.globwave.org/News/Wave-Community/New-merged-altimeter-database-just-released), a database that has merged, recalibrated and reprocessed 20 years of satellite data to yield homogenous daily data sets. Buoy data are obtained from http://www.ndbc.noaa.gov/ .

4.2 Test Areas and Observations

Satellite altimeter observations are the primary source of "ground truth" in this section, but waveheight observations from four buoys are also included. The model is compared against:

- altimeter data (H_{m0} and U_{10}) globally, with both a spatial distribution of statistics and an overall distribution of the statistics presented. Four altimeters are used: ERS-2, Envisat, Jason-1, and Jason-2.
- altimeter data (H_{m0}) near NOAA NDBC buoy 46006. This is done to confirm that statistics from comparison against buoy data are consistent with statistics from comparison against satellite data
- buoy data bulk parameters (H_{m0} and U_{10}) from limited deepwater locations including NOAA NDBC buoys 46006, 41001, 41010, 41048. Note that the last buoy, 41048, is also used in Section 3 (see Table 3-3).

The statistics used in this study include:

- correlation coefficient (denoted as "r" or "CC"). This is sometimes referred to as "Pearson's correlation coefficient" and is computed as: $\mathrm{CC} = \frac{\langle (O-\bar{O})(M-\bar{M}) \rangle}{\sqrt{\langle (O-\bar{O})^2 \rangle}\sqrt{\langle (M-\bar{M})^2 \rangle}}$, where $\bar{}$ and $\langle \ \rangle$ indicate a mean, O are observations and M are model values.
- bias (i.e. mean error),
- RMSE (root mean square error),
- NRMSE (normalized RMSE as defined by Ardhuin et al. (2010)), $\mathrm{NRMSE} = \sqrt{\frac{\sum (O-M)^2}{\sum O^2}}$
- slope (linear regression slope where regression passes through the origin, *y*-intercept=0), and
- SI (scatter index). SI is defined here as the RMSE divided by the mean of the observations. Note that some authors define this slightly differently, as the standard deviation of the errors

(i.e. demeaned RMSE) divided by the mean of the observations. Also note that this quantity is similar to the NRMSE.

The methods used to compare the model results with altimeter data are as follows. First, we matched them in time and space. For a given hourly computed global WW3, we selected altimeter wave data acquired within 30 minutes of model time. We then spatially interpolated WW3 hourly results into the track locations of selected altimeter data. This process was repeated for all hourly WW3 outputs to match WW3 and altimeter data for the entire WW3 model prediction time period.

The next step was to sort and compute the data. We regrouped and divided the temporally and spatially matched global WW3 and altimeter data into smaller cells (2 by 2° of longitude and latitude). For each cell, we carried out comparisons between the grouped WW3 and altimeter waves by computing selected statistical variables (correlation coefficient, mean bias, RMSE, linear slope, etc.) The computed statistics were then associated with the center location of each cell and could easily be displayed graphically.

4.3 Model Setup

Major characteristics of the model were as follows:

- 0.5° geographic resolution (720 longitudes and 361 latitudes) on a regular grid. Latitudes 78N to 90N and 78S to 90S are excluded from the computational grid via masking, so only 311 latitudes are actually computed. There are 155k sea points.
- 36 directional bins (10° resolution), [-5, 5, 15, …]
- 25 frequency bins, with logarithmic spacing from 0.0418 to 0.4117 Hz (increment factor = 1.1).
- The experiment was conducted over four months, from 0000 UTC 1 September 2010 to 0000 UTC 1 January 2011. The first week was treated as a period of ‘spin-up’. Excluding this period, the effective duration available for validation was 115 days total.

Minor characteristics of the model:

- a global time step of 3600 s and a time step for x/y propagation at 480 s.
- Joint North Sea Wave Project (JONSWAP) bottom friction with gamma = 0.038.
- surf breaking, Miche limiter, bottom scattering, and triad interactions were not active.
- Seeding was used in place of linear wind input.
- The default settings were used for propagation, with an averaging method employed to address the anti-Garden Sprinkler Effect (Tolman 2003).
- An obstruction map was used for sub-grid blocking (Tolman 2003). This was provided by Paul Wittmann (FNMOC).
- Bathymetry was also provided by Paul Wittmann. In this bathymetry, latitudes 78N to 90N and 78S to 90S are given as land.
- Ice concentrations greater than 75% were treated as land. Ice concentrations less than 25% were treated as open ocean. Otherwise, partial sub-grid blocking was used, as described by Tolman (2003).
- Water levels and currents are not included.

- Data assimilation is not included.
- Minimum water depth for computations is 2.5 m.

For the source term test denoted as ST2, the model was run with Tolman and Chalikov (1996) physics with default settings. The ST4 test was run with Ardhuin et al. (2010) physics with default settings.

To permit use of the ST4 physics, version 4 of the model is used. To check consistency with v3.14 for the ST2 physics, a test simulation was performed (not presented). Model output was compared (v3 vs. v4) at buoy locations. This revealed major discrepancies, which led to some debugging of version 4 by NRL. The bug was found and corrected. The test was repeated and the remaining discrepancies were found to be trivial.

The wind forcing tests were made with the model using two sources of wind data. The first came from the NCEP Climate Forecast System Reanalysis (CFSR). The CFSR was completed over a 31-year period of 1979 to 2009 and then extended using NCEP's Climate Forecast System Version 2 (CFSv2) (Saha et al. (2010)). The wind and ice fields are on an irregular grid known as a Gaussian grid with dimensions n_i=1152, and n_j=576. They are provided in grib2 (binary) format. The time interval between fields is 1 hour.

The second source of wind data was NOGAPS winds (Hogan and Rosmond 1991). These winds are given on the same grid as WW3, at 0.5° resolution with a 3 hour interval.

Global ice concentrations were not available in our NOGAPS archives. Associated archives for the Arctic were available, but preliminary experiments with global hindcasts omitting ice around Antarctica produced unacceptable results. Therefore, we use the global CFSR ice fields for all simulations.

The run time varied between 4 and 15 hours using 48 processors on a local Linux cluster with non-uniform hardware capabilities. Run time variability seemed to be due more to hardware variability and/or competition for these resources than with model setup differences. Based on prior experience with single-machine simulations, we know that ST4 physics tends to take more computation time than ST2 physics. Computations times on the Linux cluster did not indicate this trend; we believe that they do not give reliable indication of future performance: testing in a controlled environment very similar to the target environment would be needed.

4.4 Results

Results are presented in figures and tables below and are organized as follows:

1. comparison to altimeter data globally, wind speed and waveheight: Figures 4-1 to 4-8 and Tables 4-1 and 4-2.
2. comparison to altimeter data at a buoy location (46006), waveheight only: Figure 4-9 and Table 4-3
3. comparison to buoy data, wind speed and waveheight: Figures 4-10 to 4-17 and Tables 4-4 to 4-11.

Comparison (2) is performed to verify the usefulness of the French Research Institute for Exploitation of the Sea (IFREMER) altimeter database for model validation.

With respect to U_{10}, CFSR winds appear to be more accurate than NOGAPS winds (Figure 4-1) when compared to altimeter data. NOGAPS over-predicts lower wind speeds and under-predicts wind speeds over 10 m/s.

Comparing model winds to the altimetry, NOGAPS has a bias of 1.1 m/s, while CFSR has a bias of 0.56 m/s. Comparing model SWH to the altimetry, WW3 with NOGAPS had mean biases of 2 and 10 cm, and the CFSR-forced WW3 simulation had a bias of 45 and 32 cm. In other words, WW3 is actually more accurate using the less accurate (NOGAPS) winds. This is not particularly surprising, since WW3 is calibrated for operational runs using winds that may be similar to NOGAPS in terms of bias trend. It has been pointed out (Arun Chawla, personal communication) that this sensitivity to bias (or lack of bias) in winds can be compensated via the "β_{max}" parameter available (this applies to the ST4 physics only). The default value of $\beta_{max} = 1.52$ is used here. In a recent study, NCEP changed this parameter to 1.37 when using CFSR winds (Arun Chawla, personal communication). The reader is also referred to Ardhuin et al. (2011a), where $\beta_{max} = 1.33$ is used with CFSR winds.

ST4 physics typically result in better statistics than ST2, but the difference is not great. This might be expected, since ST2 has been used with great success globally during the last decade, as noted in the NCEP references in Section 2.1. However, this is in contrast to the Lake Michigan application of Ardhuin et al. (2010) in which ST4 was clearly superior. There is insufficient evidence to make strong conclusions, but we believe the evidence points to the following situation: 1) without re-tuning, ST2 is less suitable for small-scale applications (e.g. Lake Michigan) than ST4, and 2) for larger-scale applications (e.g. Gulf of Mexico, or global) the source terms packages are of roughly similar skill, with ST4 giving a slight improvement.

In the overall probability distribution function (pdf) (Figure 4-2), there is a kink in the ST4 distributions not seen in the ST2 distributions (contours are more elliptical in the two ST2 plots). Similar, in the waveheight histograms, looking at the cases with NOGAPS forcing, with ST2, the bias for H_{m0} between 2 and 3 m is small. With ST4, there is a positive bias for $H_{m0}\sim 2$ and negative bias for $H_{m0}\sim 3$. The cause of this was initially not known. However, per information provided by Dr. F. Ardhuin (IFREMER, France), we now know that this is caused by the swell dissipation scheme (Ardhuin et al. 2010). Following a Reynolds number calculation, this scheme applies a dissipation that is based on an assumption of either laminar or turbulent boundary layer in the air above the waves. This either/or (laminar/turbulent) scheme results in the anomaly in the ST4 distributions visible here. According to Dr. Ardhuin, this feature has been corrected in a new version of the code, available in the WW3 trunk on the NCEP repository at time of writing but not yet applied by NRL. The correction involves creating an artificial, smooth transition between laminar and turbulent boundary layer dissipation. In the context of the naming convention used by Ardhuin et al. (2010), the sudden transition is a symptom of the "TEST441" physics used here. The new scheme with the smoothed transition is now being referred to as "TEST451" physics.

In the tropics, ST4 is less energetic than ST2. In some cases, this results in smaller bias (e.g. offshore of Peru, where ST2 has a positive bias). In other cases, this results in larger bias (e.g. central Pacific, where ST4 has bands of negative bias near 8°N and 10°S).

In the context of the anecdotal reports from the fleet of overprediction of swell by the FNMOC WW3, the fact that ST4 is less energetic than ST2 in the tropics can be considered a positive feature of ST4.

NCEP has been using ST4 (TEST 451) physics since late May 2012. They report that bias in swell is largely addressed via the new physics but that a negative bias exists in some regions of wave generation, off the Asian coasts, and the US east coast. (Chawla, personal communication)

As was mentioned above, the altimeter SWH near a particular buoy (46006, over 1000 km west of Eureka, CA) is compared to the model, mimicking a comparison between the model and data from that buoy. This is done to verify the usefulness of the IFREMER altimeter database for model validation. The outcome improves confidence in the IFREMER database: in both cases, the CFSR-forced models have positive bias (more than 33 cm), and both NOGAPS-forced models have a weaker negative bias (less than 19 cm); the actual values of bias are quite similar between Figure 4-9 and 4-10. The worst RMSE occurs with ST2-CFSR and the best RMSE with ST4-NOGAPS. In the altimeter vs. model comparison, the best correlation (C.C. or *r* parameter) is with the ST4 physics. In the buoy vs. model comparison, the best correlation is with the NOGAPS-forced ST4 model. However, as mentioned above, the difference between physics packages is modest for this large-scale model application.

Table 4-1: Statistical comparisons of U_{10} wind speed for CFSR and NOGAPS models with altimeter observations.

Winds speed – Models vs. Altimeter Observations					
Model used for wind forcing	**N**	**CC**	**Bias**	**RMSE**	**Slope**
CFSR	16×10^6	0.90	0.56 m/s	1.76 m/s	0.93
NOGAPS		0.91	1.1 m/s	1.92 m/s	0.87

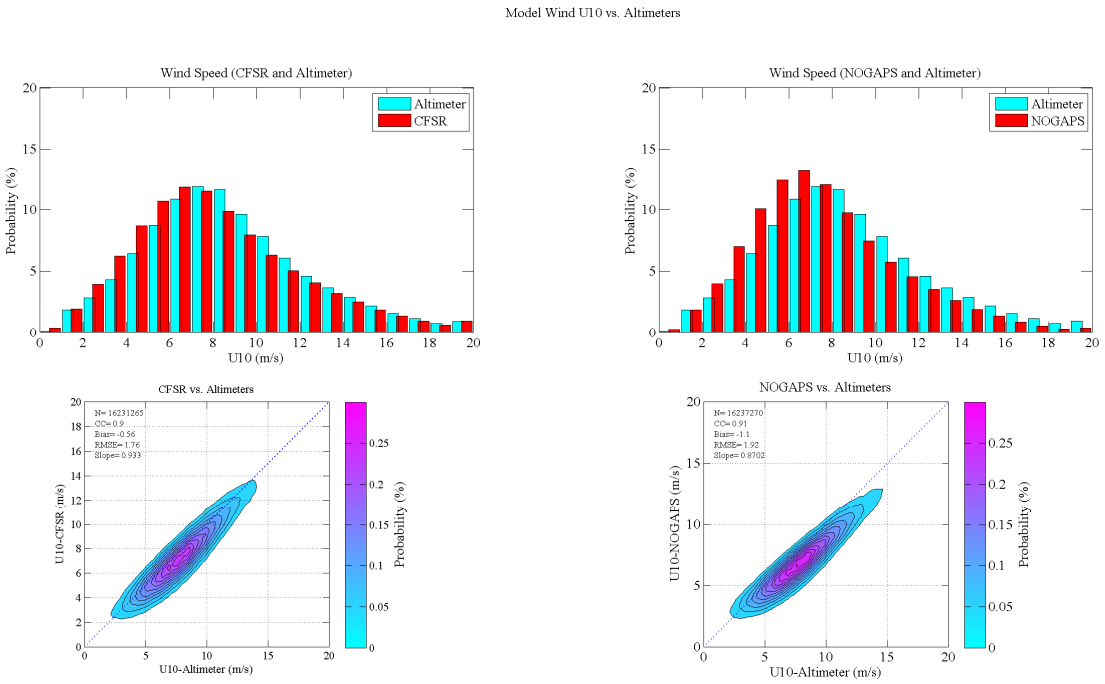

Figure 4-1: WW3 U_{10} wind speed probability: CFSR (left) and NOGAPS (right) compared to altimeter winds.

Table 4-2: Significant wave height statistics comparing CFSR and NOGAPS model runs with altimeter data.

SWH statistics comparing WW3 vs. Altimeter Observations					
Source term package and wind forcing	**N**	**CC**	**Bias**	**RMSE**	**Slope**
ST2 – CFSR	16×10^6	0.95	0.45 m	0.67 m	1.15
ST2 – NOGAPS		0.95	-0.02 m	0.44 m	0.98
ST4 – CFSR		0.96	0.32 m	0.60 m	1.12
ST4 – NOGAPS		0.96	-0.10 m	0.41 m	0.96

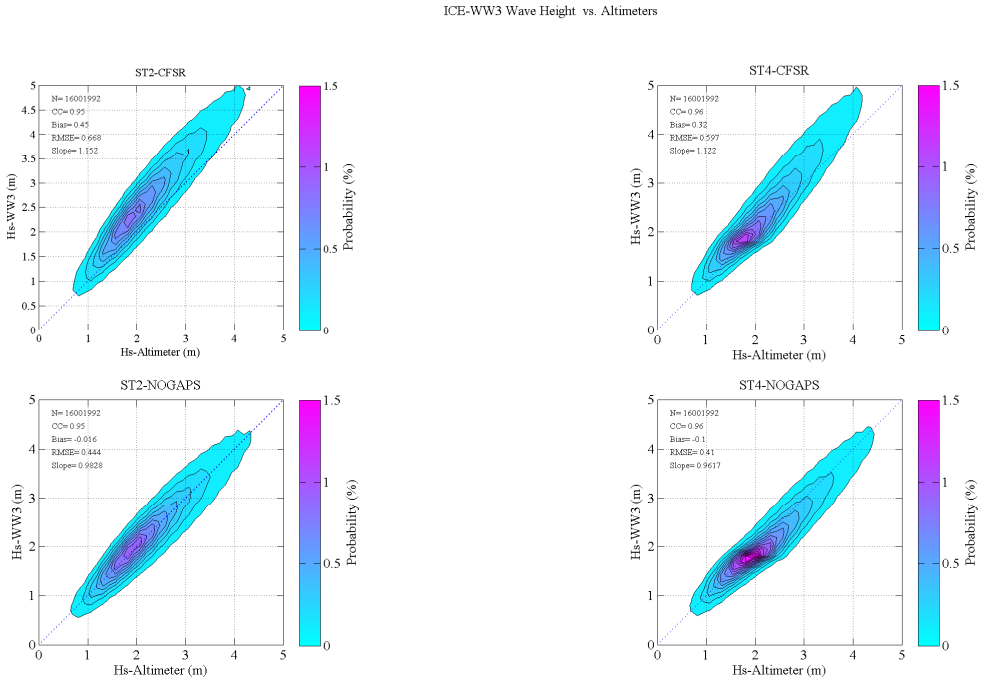

Figure 4-2: SWH (m) contoured probability plots for WW3 with: wind forcing from CFSR (upper plots); wind forcing from NOGAPS (lower plots); ST2 physics (left); ST4 physics (right).

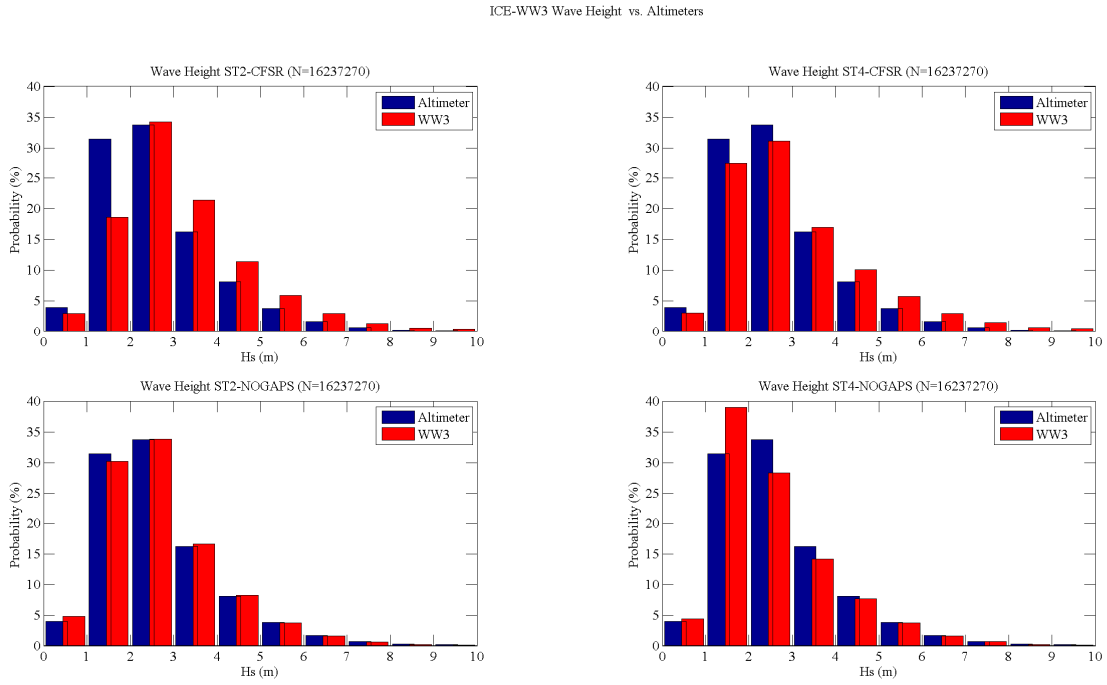

Figure 4-3: SWH probability, comparing WW3 and altimeter data with: wind forcing from CFSR (upper plots); wind forcing from NOGAPS (lower plots); ST2 physics (left); ST4 physics (right).

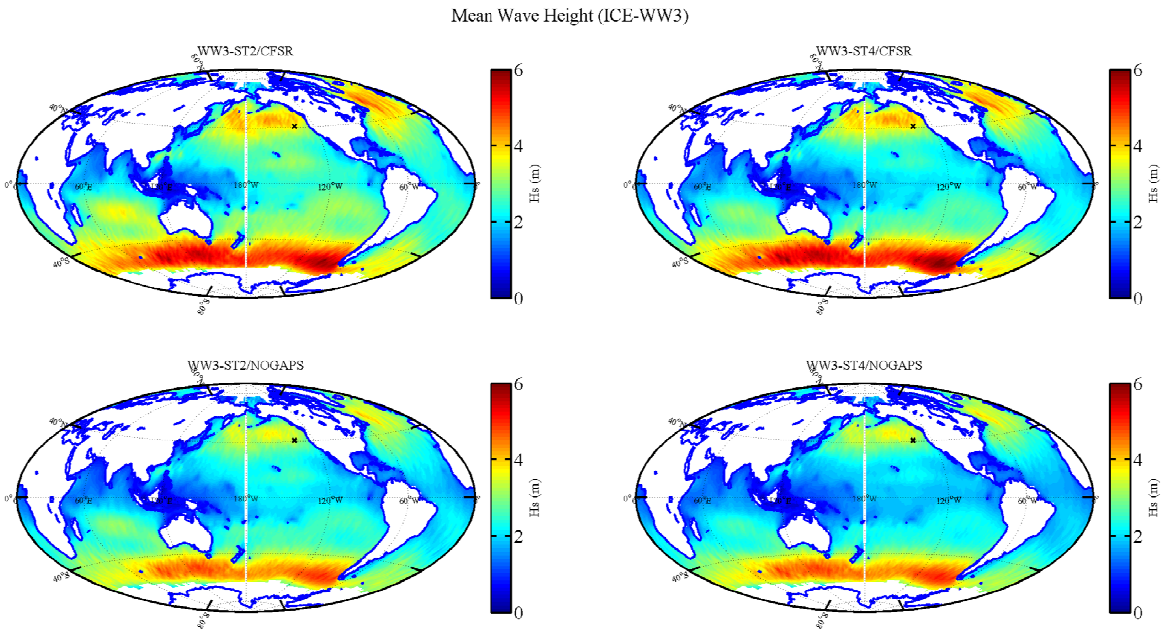

Figure 4-4: Mean of significant wave height (m) for hindcast duration, with wind forcing from CFSR (upper plots); wind forcing from NOGAPS (lower plots); ST2 physics (left); ST4 physics (right) and ST4 (left).

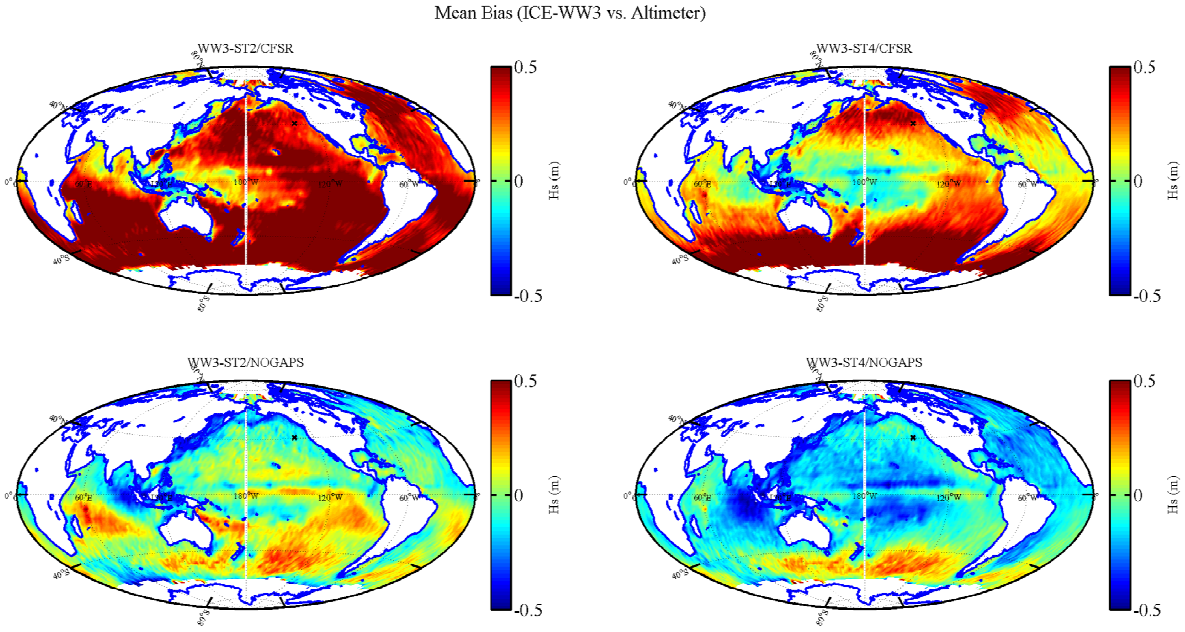

Figure 4-5: SWH mean bias WW3 vs. altimeter data, with wind forcing from CFSR (upper plots); wind forcing from NOGAPS (lower plots); ST2 physics (left); ST4 physics (right).

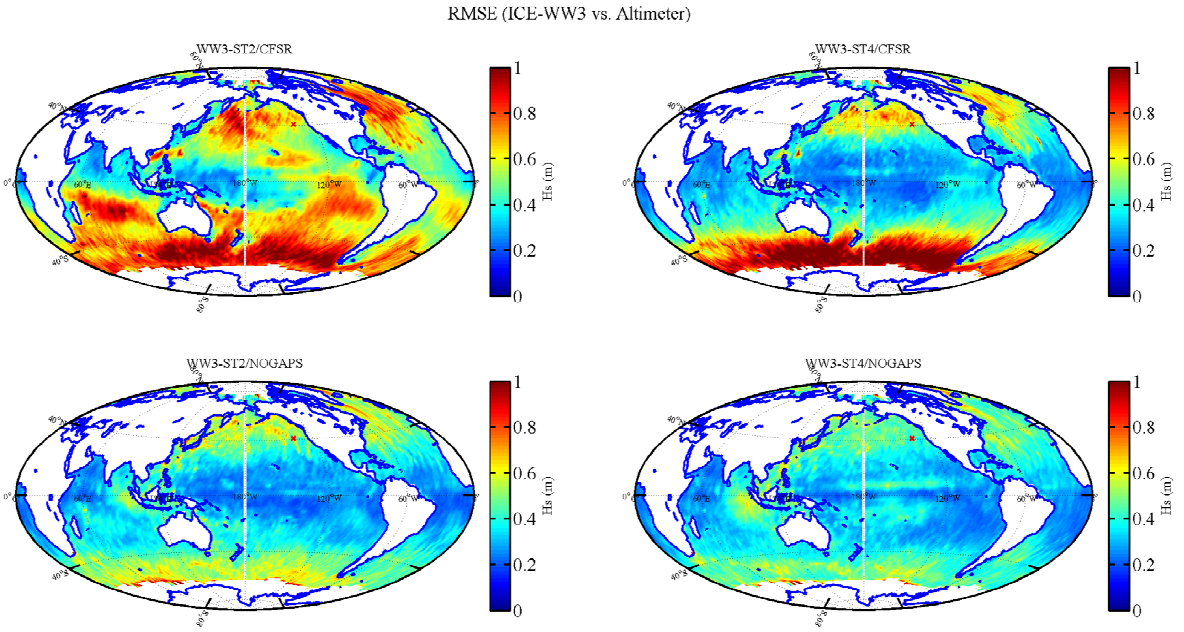

Figure 4-6: SWH RMSE WW3 vs. altimeter data, with: wind forcing from CFSR (upper plots); wind forcing from NOGAPS (lower plots); ST2 physics (left); ST4 physics (right).

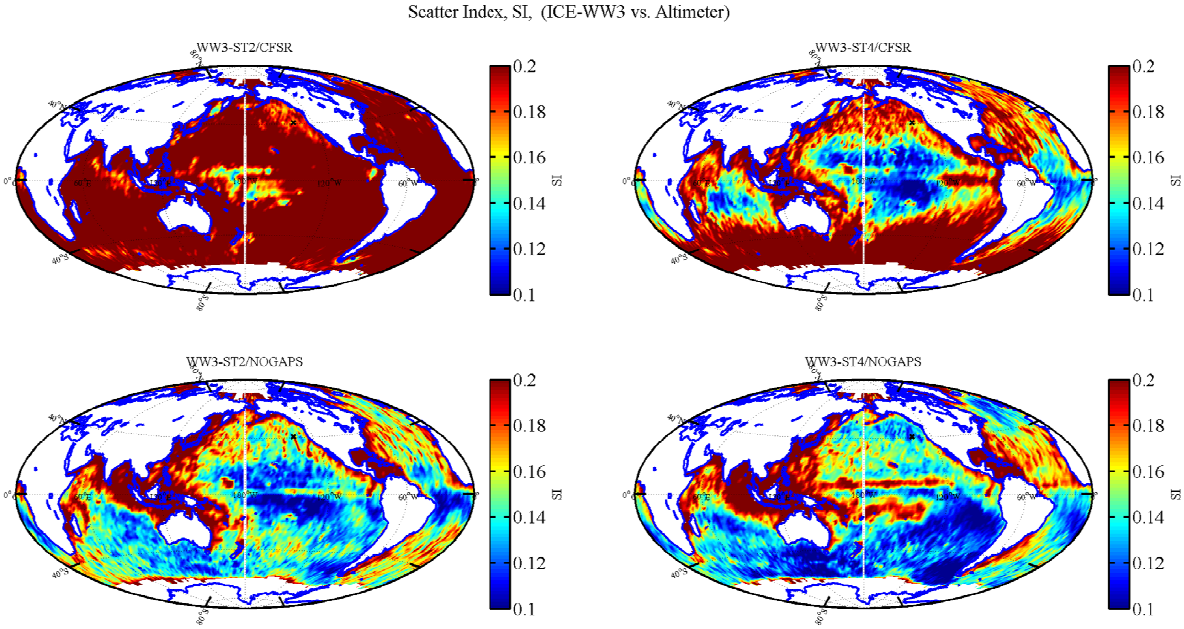

Figure 4-7: SWH Scatter Index WW3 vs. altimeter data, with: wind forcing from CFSR (upper plots); wind forcing from NOGAPS (lower plots); ST2 physics (left); ST4 physics (right).

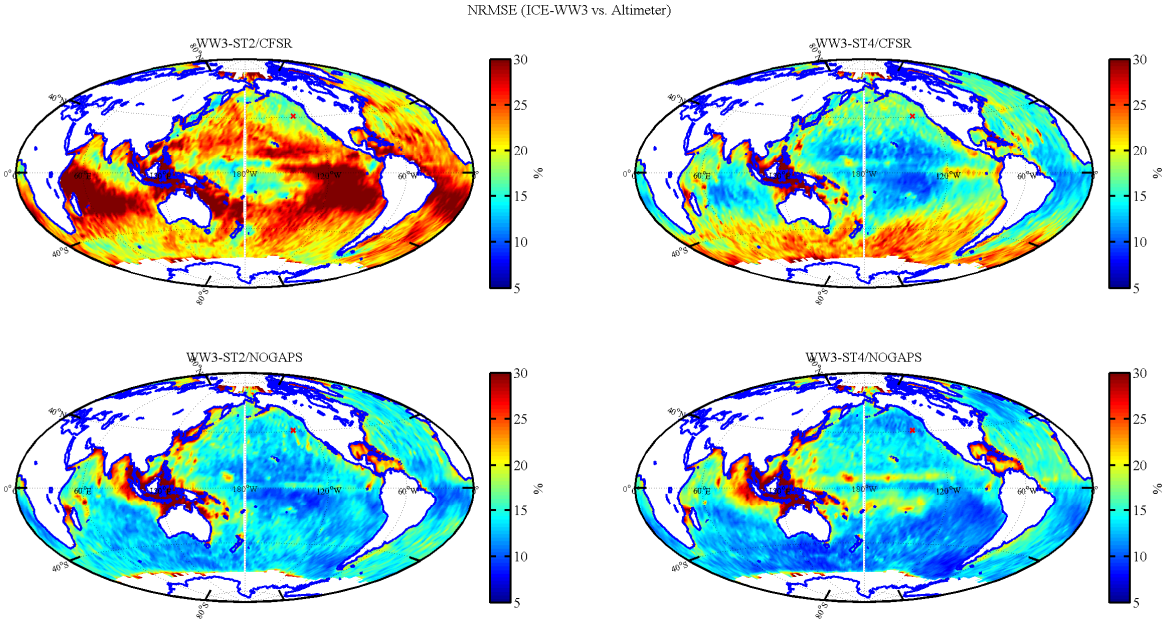

Figure 4-8: SWH normalized RMSE WW3 vs. altimeter data, with: wind forcing from CFSR (upper plots); wind forcing from NOGAPS (lower plots); ST2 physics (left); ST4 physics (right).

Table 4-3: Statistical comparison of SWH near buoy 46006 for WW3 vs. altimeter observations.

SWH (m) near buoy 46006 — WW3 vs. altimeter 2x2° cell					
Source term package and wind forcing	**N**	**CC**	**Mean Bias**	**RMSE**	**Slope**
ST2 – CFSR	1849	0.92	0.37 m	0.60 m	1.09
ST2 – NOGAPS	1849	0.91	-0.15 m	0.52 m	0.94
ST4 – CFSR	1849	0.94	0.35 m	0.56 m	1.09
ST4 – NOGAPS	1849	0.94	-0.18 m	0.45 m	0.93

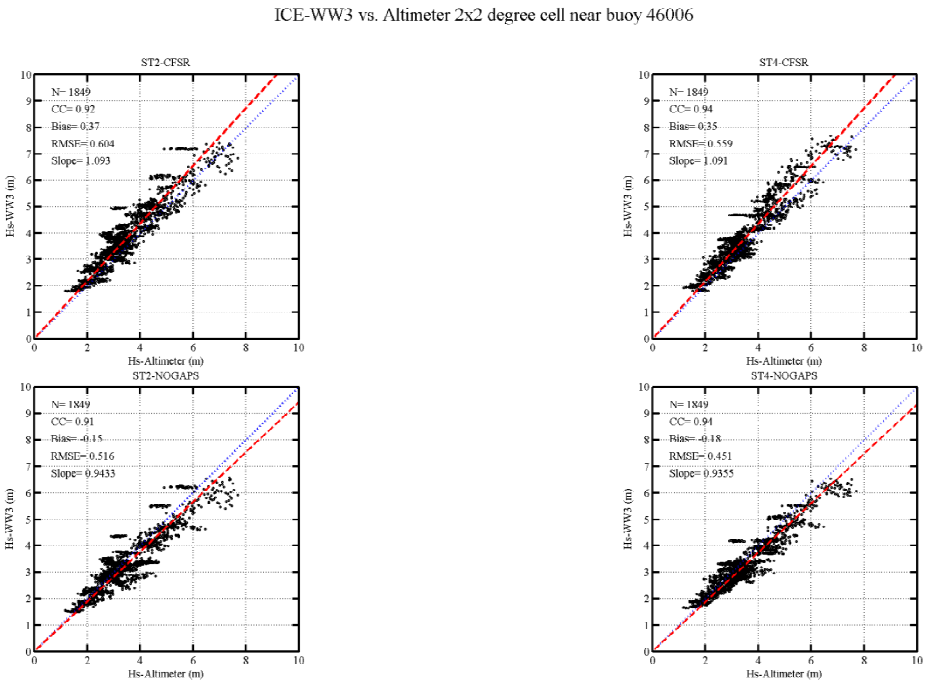

Figure 4-9: SWH near buoy 46006 WW3 vs. altimeter data (2x2° cell); ST2 using CFSR and NOGAPS wind forcing (left), ST4 (right).

Table 4-4: Significant wave height at buoy 46006, comparing WW3 against buoy.

Model vs. buoy SWH (m) at buoy 46006					
Source term package and wind forcing	**N**	**CC**	**Mean Bias**	**RMSE**	**S.I.**
ST2 – CFSR	2458	0.94	0.34 m	0.58 m	0.18
ST2 – NOGAPS	2458	0.93	-0.13 m	0.50 m	0.15
ST4 – CFSR	2458	0.94	0.34 m	0.57 m	0.18
ST4 – NOGAPS	2458	0.95	-0.14 m	0.44 m	0.13

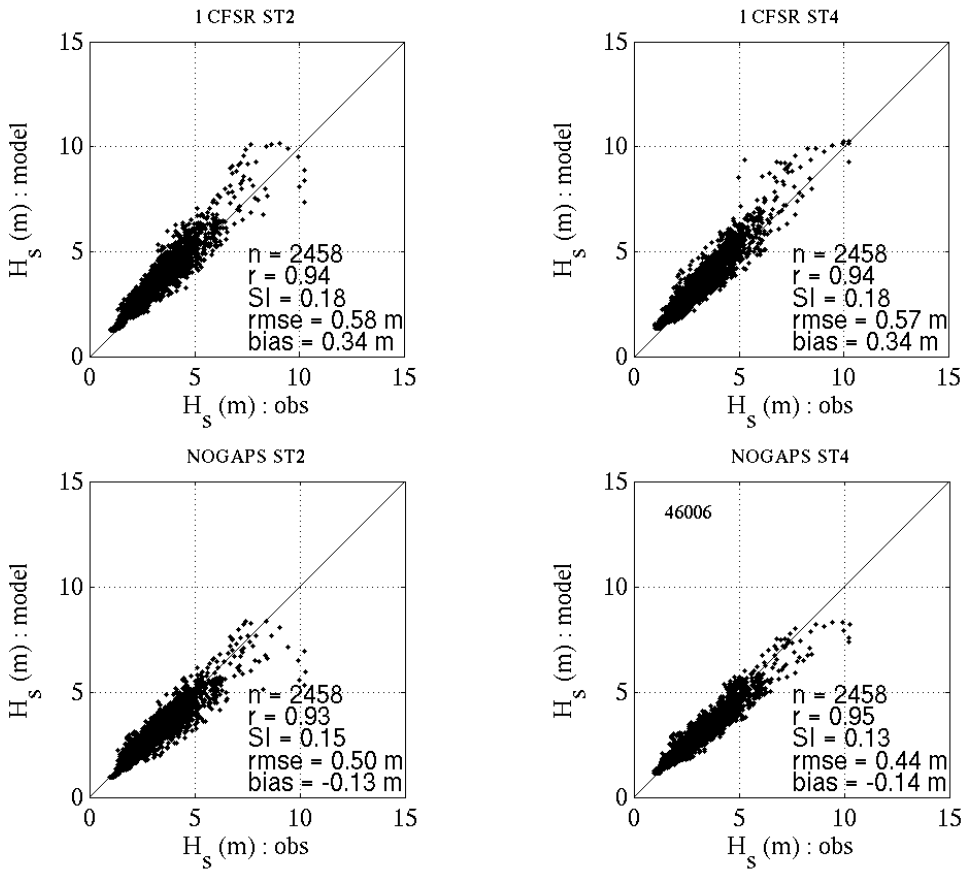

Figure 4-10: Significant wave height at buoy 46006 scatter plot comparison of model vs. buoy observations.

Table 4-5: Significant wave height at buoy 41001, comparing WW3 against buoy.

Model vs. buoy SWH (m) at buoy 41001					
Source term package and wind forcing	**N**	**CC**	**Mean Bias**	**RMSE**	**S.I.**
ST2 – CFSR	2748	0.93	0.17 m	0.59 m	0.23
ST2 – NOGAPS	2748	0.95	-0.21 m	0.55 m	0.22
ST4 – CFSR	2748	0.96	0.08 m	0.45 m	0.18
ST4 – NOGAPS	2748	0.97	-0.23 m	0.51 m	0.20

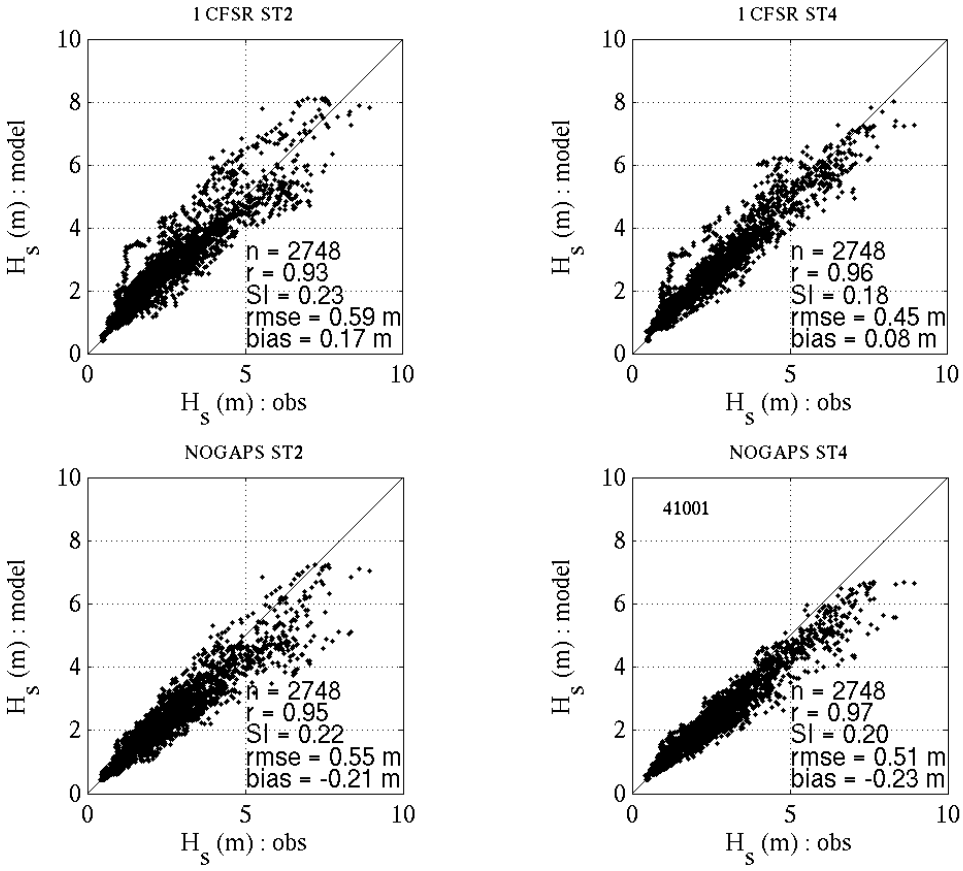

Figure 4-11: Significant wave height at buoy 41001 scatter plot comparison of model vs. buoy observations.

Table 4-6: Significant wave height at buoy 41010, comparing WW3 against buoy.

Model vs. buoy SWH (m) at buoy 41010					
Source term package and wind forcing	**N**	**CC**	**Mean Bias**	**RMSE**	**S.I.**
ST2 – CFSR	5518	0.92	0.24 m	0.44 m	0.25
ST2 – NOGAPS	5518	0.93	-0.03 m	0.33 m	0.19
ST4 – CFSR	5518	0.94	0.09 m	0.32 m	0.18
ST4 – NOGAPS	5518	0.95	-0.11 m	0.31 m	0.18

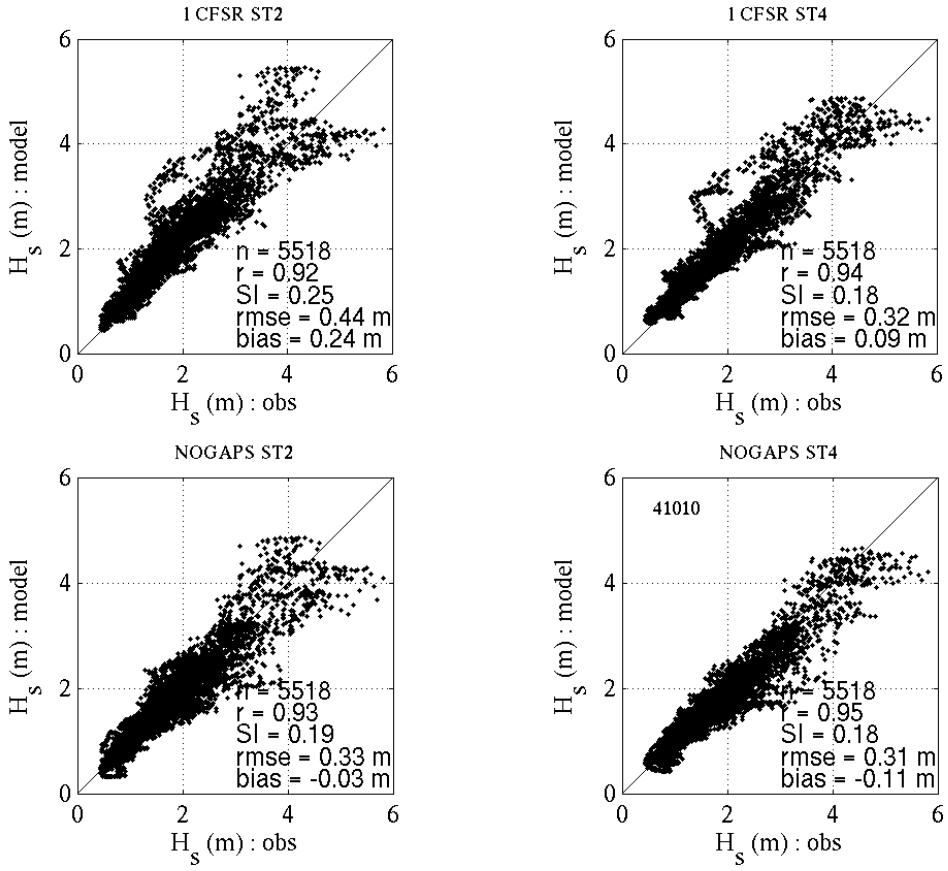

Figure 4-12: Significant wave height at buoy 41010 scatter plot comparison of model vs. buoy observations.

Table 4-7: Significant wave height at buoy 41048, comparing WW3 against buoy.

Model vs. buoy SWH (m) at buoy 41048					
Source term package and wind forcing	**N**	**CC**	**Mean Bias**	**RMSE**	**S.I.**
ST2 – CFSR	2741	0.95	0.34 m	0.61 m	0.24
ST2 – NOGAPS	2741	0.97	-0.03 m	0.40 m	0.16
ST4 – CFSR	2741	0.97	0.17 m	0.43 m	0.17
ST4 – NOGAPS	2741	0.98	-0.14 m	0.39 m	0.15

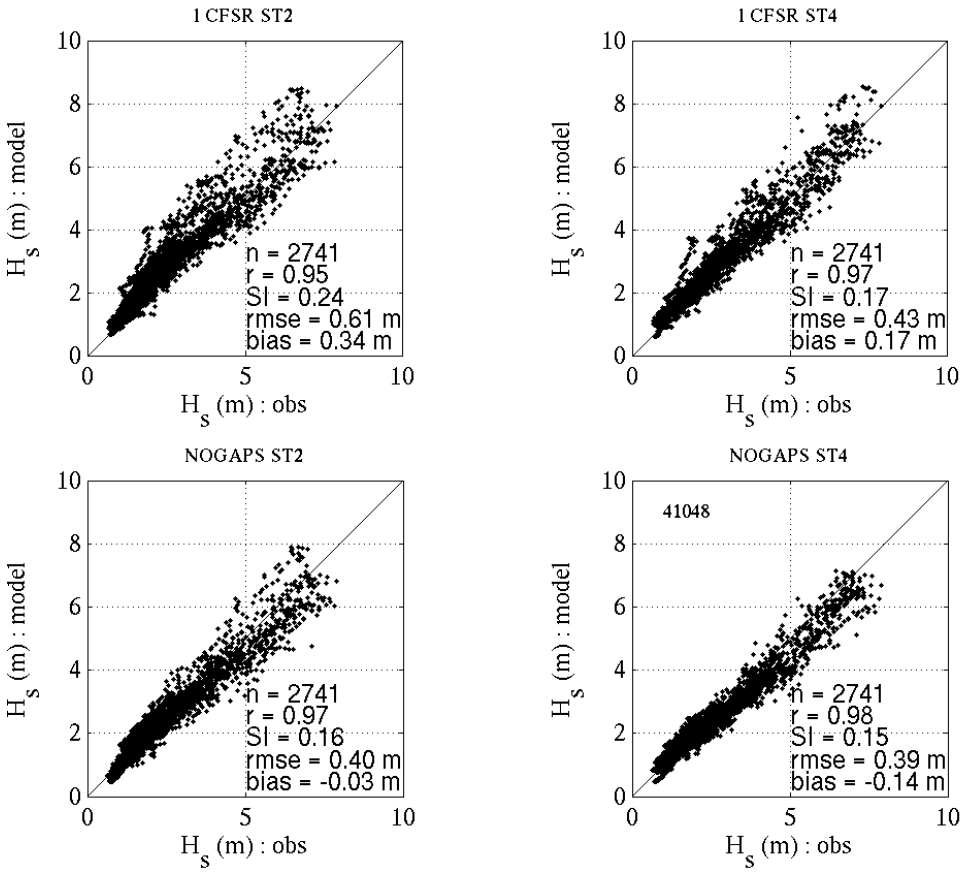

Figure 4-13: Significant wave height at buoy 41048 scatter plot comparison of model vs. buoy observations.

Table 4-8: Wind speed at buoy 46006, comparing WW3 against buoy.

Model vs. buoy U_{10} (m/s) at buoy 46006					
Source term package and wind forcing	**N**	**CC**	**Mean Bias**	**RMSE**	**S.I.**
ST2 – CFSR	2736	0.92	0.42 m/s	1.57 m/s	0.19
ST2 – NOGAPS	2736	0.92	-0.01 m/s	1.38 m/s	0.17

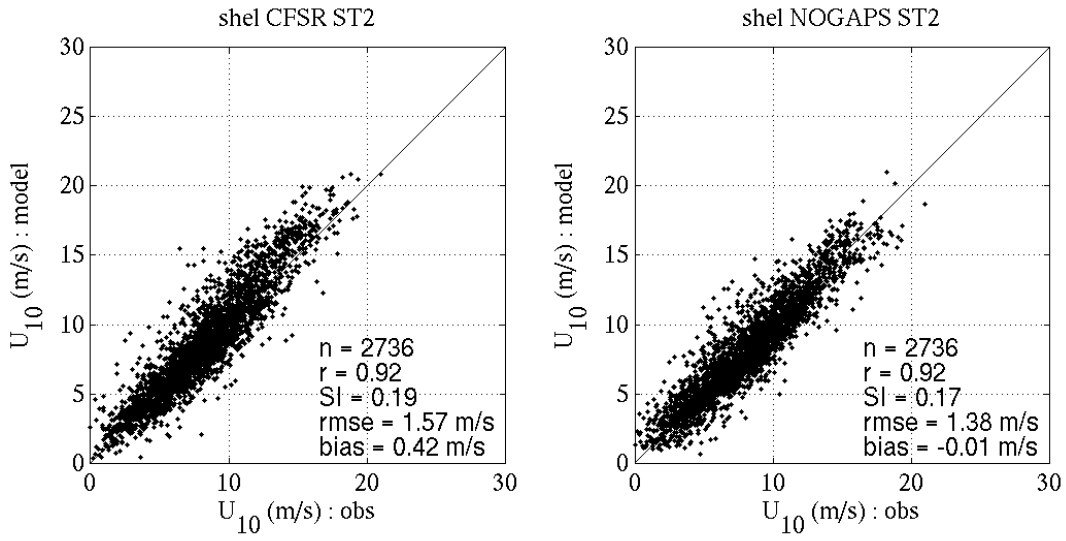

Figure 4-14: Wind speed at buoy 46006 scatter plot comparison of model vs. buoy observations.

Table 4-9: Wind speed at buoy 41001, comparing WW3 against buoy.

Model vs. buoy U_{10} (m/s) at buoy 41001					
Source term package and wind forcing	**N**	**CC**	**Mean Bias**	**RMSE**	**S.I.**
ST2 – CFSR	2758	0.94	-0.17 m/s	1.47 m/s	0.16
ST2 – NOGAPS	2758	0.93	-0.43 m/s	1.56 m/s	0.17

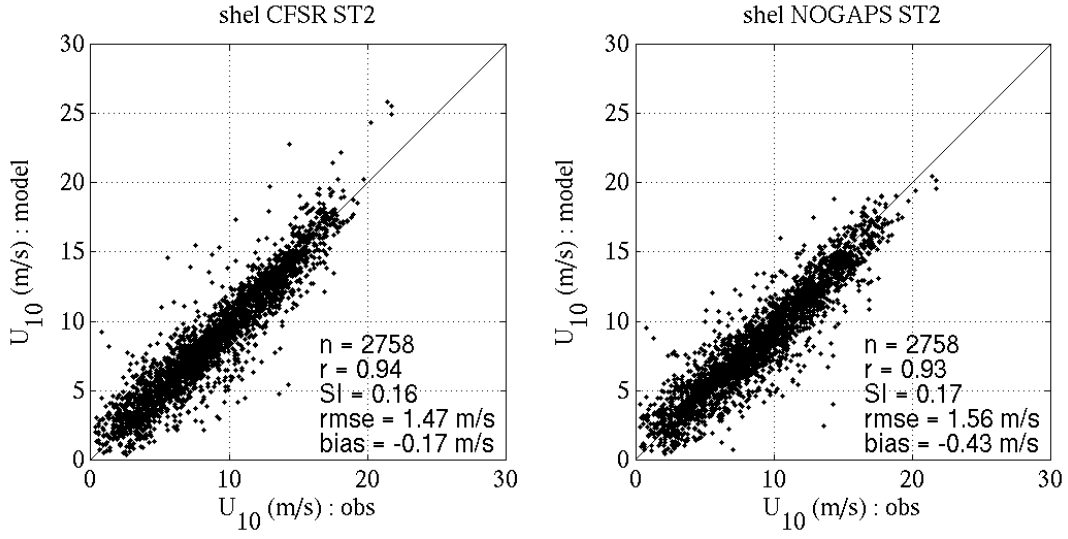

Figure 4-15: Wind speed at buoy 41001 scatter plot comparison of model vs. buoy observations.

Table 4-10: Wind speed at buoy 41010, comparing WW3 against buoy.

Model vs. buoy U_{10} (m/s) at buoy 41010					
Source term package and wind forcing	**N**	**CC**	**Mean Bias**	**RMSE**	**S.I.**
ST2 – CFSR	5519	0.93	-0.16 m/s	1.25 m/s	0.18
ST2 – NOGAPS	5519	0.91	-0.16 m/s	1.42 m/s	0.21

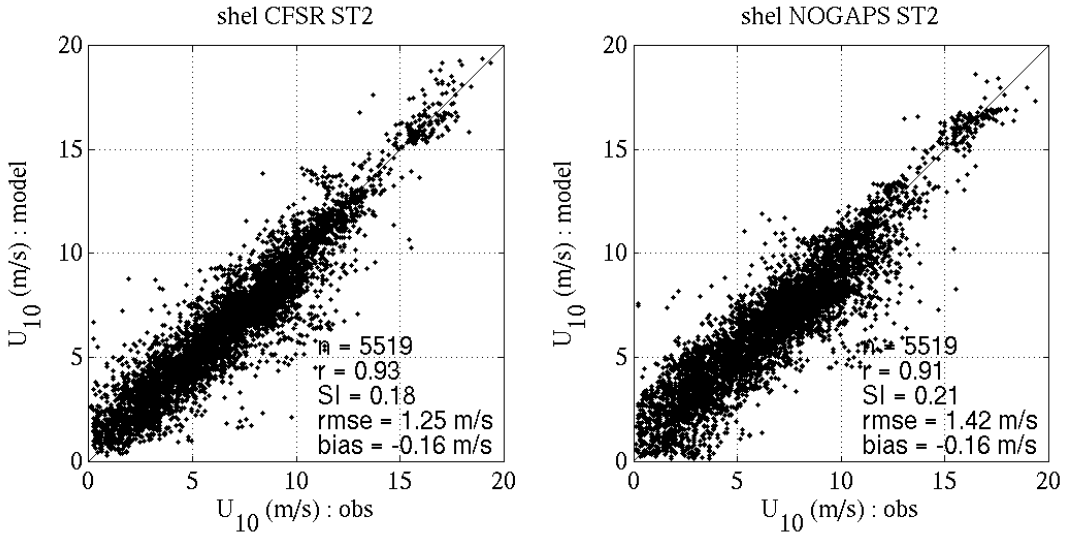

Figure 4-16: Wind speed at buoy 41010 scatter plot comparison of model vs. buoy observations.

Table 4-11: Wind speed at buoy 41048, comparing WW3 against buoy.

Model vs. buoy U_{10} (m/s) at buoy 41048					
Source term package and wind forcing	**N**	**CC**	**Mean Bias**	**RMSE**	**S.I.**
ST2 – CFSR	2759	0.94	-0.23 m/s	1.44 m/s	0.17
ST2 – NOGAPS	2759	0.94	-0.51 m/s	1.53 m/s	0.18

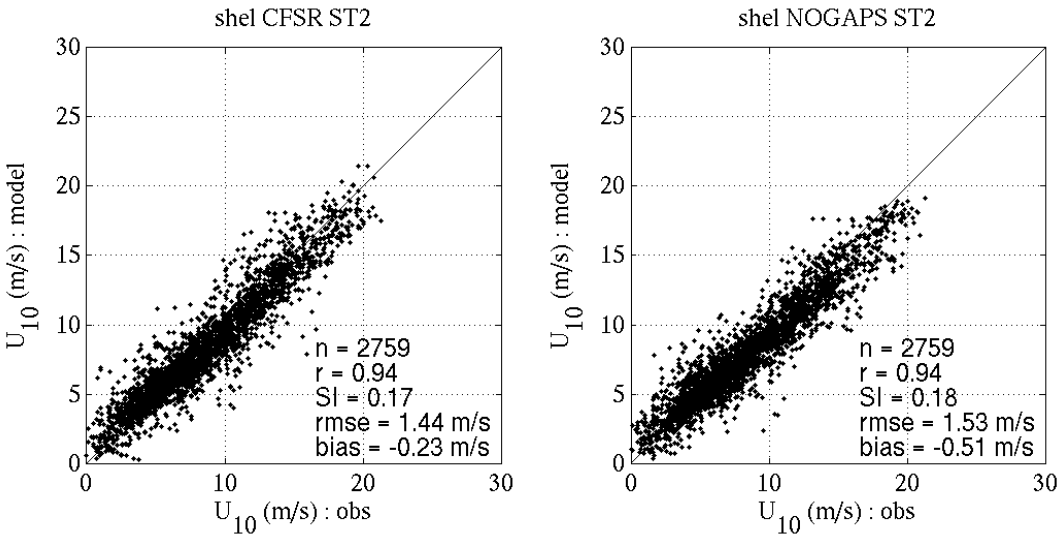

Figure 4-17: Wind speed at Buoy 41048: scatter plot comparison of model vs. buoy observations.

4.5 Conclusions

Overall, error metrics for WW3 with NOGAPS forcing are acceptable. For comparison, see accuracy of global hindcasts reported by Tolman (2002), Ardhuin et al. (2010) or Chawla et al. (2011). Statistics given in Fig. 2.2 of Tolman (2002) (all ERS-2 data used globally) are very similar to the overall statistics shown here. It might be expected that better statistics could be achieved, especially with regard to bias, by re-calibration of the source terms to better match the altimeter data here (e.g. the "β_{max}" parameter discussed above), as is done by NCEP and IFREMER for their operational model, but this is beyond the scope of the current project.

Based on these results, we recommend a) adoption of the Ardhuin et al. (2010) physics (ST4), for NAVO's operational multi-grid model, as it is modestly more skillful than the standard ST2 physics, and b) that the "TEST 451" subset of the ST4 physics be used, since we expect that corrects the known, minor problem observed in the "TEST 441" results shown here. TEST 451 is *not* available in the code being run for the real-time system (Section 3) at time of writing. Thus, the switch from ST2 to ST4 must wait until a stable version of the NCEP development code is regression-tested at NRL and built at NAVOCEANO.

5.0 DISCUSSION

Contributing author: Erick Rogers

Conclusions based on selected prior studies have been summarized in Section 2, and conclusions based on results presented in this VTR have been given in Section 3 and 4. In this section, we provide some new remarks, with particular focus on possible improvements to the system described in Section 3.

- The existing WAM system does not include ice. By using a wave model implementation that includes sea ice, we expect considerable improvement in wave predictions, especially near Antarctica. This will not have much impact on skill in comparison to a large majority of NDBC buoys, but should be quite noticeable in comparison to altimetry.
- The NAVOCEANO OPTEST should include at least some validation with altimeter data globally. NRL has some experience with this (e.g. Section 4) and is able to assist.
- As discussed in Section 3, the placeholder ice forcing file in the real-time system should be replaced with a routinely updated ice forcing file, making the ice fields non-stationary. The hindcast system in Section 4 includes non-stationary global ice fields; in that respect, it is comparable to the future real-time system, rather than the present real-time system.
- As discussed in Section 4, the future real-time system should utilize the new TEST 451 physics, whereas the existing system uses TC96 physics.
- The present system (WW3 at NAVOCEANO) does not include data assimilation. Data assimilation is performed now operationally for the FNMOC WW3 by modifying restart files by incorporating altimeter wave height observations. (Cummings 2008). This has the benefit of improving wave height predictions for nowcasts and short-term forecasts (e.g. 24 hours). With information about the spectral distribution of energy from satellite, e.g. from SAR, future data assimilation systems can potentially improve longer-term forecasts as well. (Without spectral information, the altered WW3 spectra will tend to propagate in the wrong direction, or at the wrong speed, which manifests as error in local energy of swells after these waves have dispersed over a period of days).
- Capability for irregular grids was implemented in WW3 by Rogers and Campbell (2009), and this is now in the development trunk of WW3 at NCEP, on a Subversion repository. This is ready for use right now in any WW3 system that uses traditional one-way nesting. For example, FNMOC has already beta-tested a curvilinear Arctic grid using this code, forced by their global WW3.
- However, this version (on the NCEP development trunk at time of writing) does not allow use of irregular grids within a multi-grid system. More recently (summer of 2011), NRL has updated the code to allow irregular grids within a multi-grid system. At time of writing, this capability is being merged into the development trunk of WW3 at NCEP from the NRL branch of WW3 at NCEP. This code has been extensively verified using simplified scenarios, as well as a realistic scenario of a curvilinear Arctic grid running with a global grid. However, with respect to efficiency, this code is still in “beta” state. After efficiency is addressed (a fairly straightforward task), transition of irregular grids (e.g. polar stereographic Arctic grid or Lambert conformal eastern Pacific grid) can be incorporated into operational multi-grid systems, such as the NAVOCEANO real-time system. In many cases, this will mean that WW3 grids are run on grids corresponding to the atmospheric model native grids.

- Coding for communication between irregular equal-rank grids (Tolman 2008) is not implemented at time of writing; we do not consider this to be a feature of importance operationally in the near-term, but should be done for sake of completeness.
- An irregular grid application that may be very significant near-term is the tri-polar global grid, such as is now applied with the Navy's global ocean models (Barron et al. 2007, Figure 2). This would require some additional coding to accommodate a special feature of this grid: specifically, to allow transmission of wave energy across an irregular seam in the Arctic. There would also be technical challenges associated with operating the model efficiently using MPI with a very large number of grid points, e.g. with resolution better than 0.1° globally.
- At present, none of the large-scale wave modeling at FNMOC and NAVOCEANO includes wave-current interaction. However, once the tri-polar grid global WW3 is running, including one-way coupling (currents-to-waves) should be straightforward using an existing operational circulation model. Two-way coupling would require that the appropriate coupling routines be built into the relevant models. In the context of WW3, this work is underway, building in an ESMF (Earth System Modeling Framework) layer.
- Code to create transmission grids for irregular grids would be necessary for application of a global irregular grid. NCEP will develop this code.
- Sea/swell partitioning capability exists in WW3. However, visualization of these partitions operationally is less straightforward. NCEP is beta-testing software that could be of great use in this regard. Documentation of the software, with specific consideration of end-users unfamiliar with the partitioning concept, would be necessary.
- We further point out that partitioning has a potential ancillary benefit for efficient data storage. Specifically, rather than archiving directional spectra, we can archive the partitioning results. When and where directional spectra are later required, e.g. to provide boundary forcing for a hindcast, these can be reconstructed in an approximate (but still fairly accurate) fashion from the partition data.
- Near Antarctica, is has been suggested by Ardhuin (2011b) that icebergs can have a significant impact on model comparisons to altimetry. A parameterization to deal with this has been implemented in a development version of WW3. This issue is separate from sea ice: the present transition will account for sea ice using parametric methods available in WW3 but will not address the impact of icebergs. The latter should be considered as a subsequent area of improvement.
- The Navy Global Environmental Model (NAVGEM) has been selected to be the Navy's next operational global numerical prediction system, replacing NOGAPS. At time of writing, it is in the late stages of the transition process. The implications of this change in wind forcing on the wave model should be considered soon after transition. This would be the ideal time to evaluate the β_{max} setting of the ST4 physics, for example.
- Wave steepness estimates are a product sometimes requested from the fleet. Unfortunately, this parameter is not straightforward. Because small waves tend to be very steep, the mean steepness of a wave spectrum is sometimes very high for an objectively benign sea state. The estimate should be provided in a manner that considers multiple length-scales, ranging from small length-scales relevant to operation of a zodiac, to larger length-scales, relevant to activities on the largest ships, such as ship-to-ship transfer of materiel. Directional spectra can be considered to additionally provide predictions of crossing seas and wave breaking. At time of writing, ONR and NAVSEA are supporting work to develop

sophisticated software that goes beyond simple length-scale quantification, and actually models individual ship motion (Environmental and Ship Motion Forecasting).

- WW3 version 3.14 allows implementation of so-called “coastal grids” in a multi-grid system (Tolman 2008). This is a type of regular grid (i.e. rectangular grid cells of uniform resolution) made “coastal” by masking cells a certain distance from the coast. In the NAVOCEANO real-time system, we did not implement any such grids, but this should be considered for near-future implementation, for example, to reduce the amount of deep-water sea points in our South America grid, thus making it much more efficient than the present setup. We point out that this type of grid still cannot be used practically for very high resolutions (e.g. better than 2 km) because of WW3’s conditionally stable propagation scheme; the model becomes much less efficient than SWAN (Booij et al. 1999) at these scales.
- Another capability under development at NCEP is the so-called quasi-stationary capability. At high resolutions, this method provides a compromise between the relatively rigorous time-stepping method of WW3 and the fully stationary approximation used by some models (e.g. used by SWAN as an option). The stationary approximation of SWAN allows very fast computations, e.g. arriving at a stationary solution in O(10) iterations rather than O(100) time steps. The WW3 method of stationary computation still uses the O(100) time steps to achieve a stationary solution. In the case of SWAN, the stationary assumption effectively assumes infinite duration, which introduces error, particularly for time-lagging swell arrival and for non-stationary wind forcing. The quasi-stationary capability allows the user to control the degree of computational rigor (reducing errors from this assumption) vs. speed. The method employs a kind of time-stretching so that a solution can be achieved in O(100) time steps rather than the O(1000) time steps that would actually be required to produce a multi-day forecast at high resolution with full rigor, e.g. a 3-day day forecast with a 100 second time step. The user-control referred to above is, in fact, via a variable controlling the degree to which time is stretched.
- Unstructured grids (e.g. with triangular cells) have been implemented in an experimental version of WW3 by IFREMER. The authors claim to have circumvented the traditional problem of needing to apply the model with a small time step to prevent instability at the region of the grid with highest resolution. NRL has no firsthand experience with this code, but it should be considered for inclusion in the roadmap for future wave model transitions. Realistically, the prospects for this feature likely coincide with the degree of NAVOCEANO commitment to unstructured grid circulation modeling. If, for example, NAVOCEANO were routinely creating unstructured grids for purposes of circulation modeling, this WW3 feature could “piggyback” on that effort, thus shortcutting the unstructured grid creation process, which is traditionally labor-intensive.
- For those readers inside the .navy.mil domain, we remind you that additional information can be found at https://www7320/Alvin/index.php/WAVEWATCH_III. This wiki will be updated with new information as it becomes available, e.g. on the NAVOCEANO OPTEST.

6.0 ACKNOWLEDGEMENTS

The authors gratefully acknowledge the contributions of Richard Allard (7322) and Dr. Gregg Jacobs (7320), particularly in the year-to-year NRL 6.4 project management and reporting. We thank NOAA NCEP for their development of WW3, their long-term commitment to open source philosophy, and the foresight shown in relatively recently migrating WW3 into a community code development project format. We thank our sources of observational data, including various space agencies, NOAA NDBC, Ifremer, and the GLOBWAVE project. The comments of the Validation Test Panel on this report are appreciated. In particular, we thank Dr. Arun Chawla (NCEP) for his detailed, helpful, and timely suggestions.

7.0 TECHNICAL REFERENCES

7.1 WAVEWATCH III® Software Documentation

Cummings, J, (2008). Validation Test Report for Assimilation of Altimeter Significant Wave Height Data in the WAVEWATCH III Wave Model Prediction System. NRL Report, 21pp.

Tolman, H.L, (2009). User Manual and System Documentation of WAVEWATCH III™ Version 3.14. *NOAA/NWS/NCEP Technical Note, MMAB Contribution No. 276*. 220 pp.

Tolman, H.L, (2007). Development of a multi-grid version of WAVEWATCH III Version 2.22. NCEP Technical Note. 112 pp.

Tolman, H. L., (2002a). Validation of WAVEWATCH III version 1.15 for a global domain. NCEP Tech. Note, 33 pp.

Tolman, H. L., (2002c) User manual and system documentation of WAVEWATCH-III version 2.22. NCEP Tech. Note, 133 pp.

Tolman, H. L., (2002e). Testing of WAVEWATCH III version 2.22 in NCEP's NWW3 ocean wave model suite. NOAA / NWS / NCEP / OMB Technical Note Nr. **214**: 99 pp.

Tolman, H. L., (1999a). User manual and system documentation of WAVEWATCH-III version 1.18. NOAA / NWS / NCEP / OMB Technical Note **166**, 110pp.

Tolman, H. L., (1997). User manual and system documentation of WAVEWATCH-III version 1.15. NOAA / NWS / NCEP / OMB Technical Note **151**, 97pp.

7.2 General Technical References

ALADIN International Team, (1997). The ALADIN project: Mesoscale modelling seen as a basic tool for weather forecasting and atmospheric research. *WMO Bulletin* **46**(4): 317–324.

Allard, R.A., J. Kaihatu, L.H. Hsu, and J.D. Dykes, (2002). The integrated ocean prediction system. *Oceanography*, **15**(1): 67-76.

Ardhuin, F., W.E. Rogers, A. Babanin, J.-F. Filipot, R. Magne, A. Roland, A. van der Westhuysen, P. Queffeulou, J.-M. Lefevre, L. Aouf, and F. Collard, (2010). Semi-empirical dissipation source functions for ocean waves: Part I, definitions, calibration and validations. *J. Phys. Oceanogr.* **40**: 1917-1941.

Ardhuin, F., J. Hanafin, Y. Quilfen, B. Chapron, P. Queffeulou, M. Obrebski, J. Sienkiewicz and D. Vandemark, (2011a). Calibration of the IOWAGA global wave hindcast (1991-2011) using

ECMWF and CFSR winds, in *12th International Workshop on Wave Hindcasting and Forecasting*, Kohala Coast, HI, 11 pp.

Ardhuin, F., J. Tournadre, P. Queffelou, and F. Girard-Ardhuin, (2011b). Observation and parameterization of small icebergs: drifting breakwaters in the Southern Ocean. *Ocean Modelling*, **39**:405-410. doi: 10.1016/j.ocemod.2011.03.004.

Ardhuin, F., L. Bertotti, J-R. Bidlot, L. Cavaleri, V. Filipetto, J-M Lefevre, P. Wittmann. (2007). Comparison of wind and wave measurements and models in the Western Mediterranean Sea. *Ocean Eng.* , 34: 526-541.

Barron, C.N, A.B. Kara, R.C. Rhodes, C. Rowley, L.F. Smedstad (2007). Validation Test Report for the 1/8° Global Navy Coastal Ocean Model Nowcast/Forecast System, NRL/MR/7320—07-9019, 149 pp.

Bidlot, J-R, D.J. Holmes, P.A. Wittmann, R. Lalbeharry, and H. S. Chen, (2002). Intercomparison of the Performance of Operational Ocean Wave Forecasting Systems with Buoy Data, Weather and Forecasting, **17**(2): 287–310.

Booij, N., and L. H. Holthuijsen, (1987). Propagation of ocean waves in discrete spectral wave models. *J. Comput. Phys.*, **68:** 307–326.

Booij, N., R.C. Ris, and L.H. Holthuijsen, (1999), A third-generation wave model for coastal regions, Part 1: Model description and validation. *J. Geophys. Res.* **104** (C4), 7649-7666.

Caplan, P., J. Derber, W. Gemmill, S.-Y. Hong, H.-L. Pan, and D. Parish, (1997). Changes to the 1995 NCEP operational medium range forecast model analysis/forecast system. *Wea. Forecasting*, **12,** 581–594.

Cavaleri, L., Bertotti, L., (2004). Accuracy of the modelled wind and wave fields in enclosed seas. *Tellus*, **56A**: 167–175.

Cavaleri, L., Bertotti, L., (2003). The characteristics of wind and wave fields modelled with different resolutions. *Quart. J. Royal Met. Soc*. **129**: 1647–1662.

Chao, Y.Y, and H. L. Tolman, (2000). Numerical experiments on predicting hurricane generated wind waves. Preprints, *Sixth Int. Workshop on Wave Hindcasting and Forecasting*, Monterey, CA, Environment Canada, 167–179.

Chao, Y. Y., and H. L. Tolman, (2001). Specification of hurricane wind fields for ocean wave prediction. *Ocean Wave Measurement and Analysis*, San Francisco, CA, B. L. Edge and J. M. Hemsley, Eds., ASCE, 671-679.

Chawla, A., D. Spindler, H. L. Tolman, (2011). A Thirty Year Wave Hindcast Using The Latest NCEP Climate Forecast System Reanalysis Winds, *12th International Workshop on Wave Hindcasting and Forecasting, Kohala Coast, Hawaii, HI*, 11pp., http://www.waveworkshop.org/.

Chawla, A., H.L. Tolman, J.L. Janson, E.-M. Devaliere, V.M. Gerald, (2009). Validation of a Multi-Grid WAVEWATCH III™ Modeling System, MMAB Contribution no. 281, online. http://polar.ncep.noaa.gov/mmab/papers/tn281/multi_hindanalysis.pdf.

Chawla, A., and H. L. Tolman, (2008). Obstruction grids for spectral wave models, *Ocean Modelling*, **22**: 12-25.

Chawla, A., and H. L. Tolman, (2007). Automated grid generation for WW3. NOAA / NWS / NCEP / MMAB Technical Note **254**, 71 pp.

Chen, H.S., L.D. Burroughs and H.L. Tolman, (2003). Ocean surface waves. Technical Procedures Bulletin 494. NOAA/NWS, online. http://polar.ncep.noaa.gov/mmab/tpbs/tpb-494.htm.

Courtier, P., Freydier, C. Geleyn, J.-F., Rabier, F., Rochas, M., (1991). The ARPEGE project at Me´te´o-France. In ECMWF 1991 Seminar Proceedings: Numerical Methods in Atmospheric Models. ECMWF, 9–13 September 1991. Vol. II, pp. 193–231.

Derber, J.C., D.F. Parish, and S.J. Lord, (1991). The new global operational analysis system at the National Meteorological Center. *Wea. Forecasting*, **6:** 538–547.

Dykes, J.D. and W.E. Rogers, 2011: WAVEWATCH III: Transition to Naval Operations, Ocean Waves Workshop Proceedings, University of New Orleans, November 17 2011, 4 pp.

Greenslade, D.J.M., (2001). The assimilation of *ERS-2* significant wave height data in the Australian region. *J. Mar. Syst.*, **28:** 141–160.

Grumbine, R. W., (1996). Automated passive microwave sea ice concentration analysis at NCEP. NWS/NCEP/OMB Tech. Note 120, 13 pp.

Hanson, J. L. and R. E. Jensen, (2004). Wave system diagnostics for numerical wave models. In 8th International Workshop on Wave Hindcasting and Forecasting, JCOMM Tech. Rep. **29**: WMO/TD-No.**1319**.

Hanson, J.L., B. A. Tracy, H. L. Tolman and D. Scott, (2006) Pacific hindcast performance evaluation of three numerical wave models. In 9th International Workshop on Wave Hindcasting and Forecasting, JCOMM Tech. Rep. **34**. Paper A2.

Hanson, J. L., B. A. Tracy, H. L. Tolman and R. D. Scott, (2009). Pacific hindcast performance of three numerical wave models. *J. Atm. Ocean. Tech.*, **26:** 1614-1633.

Hogan, T.F. and Rosmond, T.E., 1991. The description of the U.S. Navy Operational Global Atmospheric Prediction System's spectral forecast models. *Mon. Wea. Rev.* **119**, 1786-1815.

Holt, M. W., (1997). Assimilation of ERS-2 altimeter observations into a global wave model. Research Activities in Atmospheric and Oceanic Modelling—1997, WGNE Rep. **25**, WMO/TD-792, 8.31–8.32.

Jensen, R.E., P.A. Wittmann, and J.D. Dykes, (2002). Global and Regional Wave Modeling Activities. *Oceanography*, **15**(1): 57-66.

Kanamitsu, M., (1989). Description of the NMC global data assimilation and forecast system. *Wea. Forecasting*, **4:** 335–243.

Kanamitsu, M., J.C. Alpert, K.A. Campana, P.M. Caplan, D.G. Deaven, M. Iredell, B. Katz, H.-L. Pan, J. Sela, and G.H. White, (1991). Recent changes implemented into the global forecast system at NMC. Wea. And Forecasting, **6**: 425-435.

Ko, D.-S., (2002). NRL DBDB2 global 2-minute topography. http://www7320.nrlssc.navy.mil/DBDB2_WWW

Komen, G. J., L. Cavaleri, M. Donelan, K. Hasselmann, S. Hasselmann, and P.A.E.M. Janssen, (1994). Dynamics and Modelling of Ocean Waves. Cambridge University Press, 532 pp.

Leonard, B. P., (1979). A stable and accurate convective modeling procedure based on quadratic upstream interpolation. *Comput. Methods Appl. Mech. Eng.*, **19:** 59–98.

Leonard, B. P., (1991). The ULTIMATE conservative difference scheme applied to unsteady one-dimensional advection. *Comput. Methods Appl. Mech. Eng.*, **88:** 17–74.

Rogers, W.E., and T.J. Campbell, (2009). Implementation of Curvilinear Coordinate System in the WAVEWATCH-III Model. NRL Memorandum Report: NRL/MR/7320-09-9193, 42 pp. [Available online at http://torpedo.nrl.navy.mil/tu/ps.]

Rogers, W.E., P.A. Wittmann, D.W. Wang, R.M. Clancy, and Y.L. Hsu, (2005). Evaluations of Global Wave Prediction at the Fleet Numerical Meteorology and Oceanography Center, *Wea. Forecasting*, **20**: 745-760.

Rogers, W.E., P.A. Wittmann, D.W. Wang, M. Clancy, and L. Hsu, (2004). Evaluations of global wind prediction at Fleet Numerical Meteorology and Oceanography Center (from the perspective of a wave modeler). NRL Memo. Rep. 7320-04-8823, 15 pp.

Rogers, W.E., (2002). The U. S. Navy's Global Wind-Wave Models: An investigation into sources of error in low frequency energy predictions. NRL Formal Report 7320-02-10035, 63pp. [Available online at http://torpedo.nrl.navy.mil/tu/ps.]

Rogers, W.E., and P.A. Wittmann, (2002). Quantifying the role of wind field accuracy in the U. S. Navy's global ocean wave nowcast/forecast system. NRL Memo. Report 7320-02-8290, 26pp. [Available online at http://torpedo.nrl.navy.mil/tu/ps.]

Saha, S., et al., (2010). The NCEP Climate Forecast System Reanalysis. *Bull. Amer. Meteor. Soc.*, **91(8)**, 1015-1056. (DOI: 10.1175/2010BAMS3001.1)

Teixeira, J., and T. F. Hogan, (2002). Boundary layer clouds in a global atmospheric model: Simple cloud cover parameterizations. *J. Climate,* **15:** 1261–1276.

Tolman, H.L, (2009). User Manual and System Documentation of WAVEWATCH III^{TM} Version 3.14. *NCEP Technical Note*. 220 pp.

Tolman, H.L. (2008). A mosaic approach to wind wave modeling. *Ocean Modelling*, **25**: 35-47.

Tolman, H. L., (2006). Development of a multi-grid version of WW3. NOAA / NWS / NCEP / MMAB Technical Note **256**, 88 pp.+ Appendices.

Tolman, H. L., (2003). Treatment of unresolved islands and ice in wind wave models. *Ocean Modelling*, **5**, 219-231.

Tolman, H. L., (2002b). Alleviating the garden sprinkler effect in wind wave models. *Ocean Modelling*, **4:** 269–289.

Tolman, H.L. (2002d) Limiters in third-generation wind wave models. *Global Atmosphere and Ocean Sys.*, **8**: 67-83.

Tolman, H. L., (1998b). Validation of NCEP's ocean winds for the use in wind wave models. G*lobal Atmosphere and Ocean Syste*m, **6:** 243-268.

Tolman, H. L., (1995). On the selection of propagation schemes for a spectral wind-wave model. NWS/NCEP Office Note **411**: 30 pp. plus figures.

Tolman, H. L., (1992). Effects of numerics on the physics in a third generation wind-wave model. *J. Phys. Oceanogr.*, **22:** 1095–1111.

Tolman, H. L., (1991). A third-generation model for wind waves on slowly varying, unsteady and inhomogeneous depths and currents. *J. Phys. Oceanogr.*, **21:** 782–797.

Tolman, H. L., (1989). The numerical model WAVEWATCH: a third generation model for the hindcasting of wind waves on tides in shelf seas. *Communications on Hydraulic and Geotechnical Engineering*, Delft Univ. of Techn., ISSN 0169-6548, Rep. no. **89-2**, 72pp.

Tolman, H. L., and J.-H. G. M. Alves, (2005). Numerical modeling of wind waves generated by tropical cyclones using moving grids. *Ocean Modelling*, **9**: 305–323.

Tolman,H.L., J. H. G. M. Alves, Y.Y. Chao, (2004). A review of operational forecasting of wind generated waves by hurricane Isabel at NCEP. NOAA/NWS/NCEP/MMAB Technical Note **235**, 45pp.

Tolman, H.L., B. Balasubramaniyan, L.D. Burroughs, D.V. Chalikov, Y.Y. Chao, H.S. Chen, and V.M. Gerald, (2002). Development and implementation of wind-generated ocean surface wave models at NCEP. *Weather and Forecasting* (NCEP Notes), **17**: 311-333.

Tolman, H. L., and N. Booij, (1998). Modeling wind waves using wave number direction spectra and a variable wave number grid. *Global Atmos. Ocean Syst.*, **6:** 295–309.

Tolman, H. L., and D. V. Chalikov, (1996). Source terms in a third-generation wind wave model. *J. Phys. Oceanogr.*, **26:** 2497–2518.

Vincent, L. and P. Soille, (1991). Watersheds in digital spaces: An efficient algorithm based on immersion simulations. *IEEE Transactions of Pattern Analysis and Machine Intelligence*, **13**: 583-598.

WAMDIG, (1988). The WAM model – a third generation ocean wave prediction model, *J. Phys. Oceanogr*., **18**: 1775-1810.

Wittmann, P. A., (2001). Implementation of WAVEWATCH-III at Fleet Numerical Meteorological and Oceanography Center. *Proc. MTS/IEEE Conf. and Exposition: An Ocean Odyssey,* November 5-8, 2001, Honolulu, HI, Marine Technology Society and IEEE, 1474–1479.

Woodcock, F., and C. Engel, (2005). Operational consensus forecasts. *Wea. Forecasting*, **20:** 101–111.

Woodcock, F., and D. J. M. Greenslade, (2007). Consensus of numerical model forecasts of significant wave heights. *Wea. Forecasting*, **22**: 792–803.

8.0 NOTES

8.1 Acronyms and Abbreviations

Acronym	Description
ALADIN	Atmospheric Limited Area Wave model (French)
ANSI	American National Standards Institute
AOML	Atlantic Oceanographic and Meteorological Laboratory
ARPEGE	Action de Recherche Petite Echelle Grande Echelle atm model
ASCII	American Standard Code for Information Interchange
BC	Boundary Conditions
CC	Correlation Coefficient
COAMPS	Coupled Ocean Atmosphere Mesoscale Prediction System
COARDS	Cooperative Ocean/Atmosphere Research Data Service
CPU	Central Processing Unit
CFSR	Climate Forecast System Reanalysis
DoD	Department of Defense
DSRC	DoD Supercomputing Resource Center
ECMWF	European Center for Medium-range Weather Forecasts
ERS-1/2	European Remote Sensing satellite
FNMOC	Fleet Numerical Meteorology and Oceanography Center
GDAS	Global Data Assimilation System
GFDL	Geophysical Fluid Dynamics Laboratory
GFS	Global Forecasting System
GOES	Geostationary Operational Environmental Satellite
GrADS	Grid Analysis and Display System
GRIB	GRIdded Binary
GTS	Global Telecommunication System
HPC	High Performance Computing
IFREMER	French Research Institute for Exploitation of the Sea
JONSWAP	Joint North Sea Wave Project
MAE	Mean Absolute Error
MB	MegaByte

Acronym	Description
MB	Mean Bias
MPI	Message Passing Interface
MRF	Medium-Range Forecast system
NAH	North Atlantic Hurricane model
NASA	National Aeronautics and Space Administration
NAVOCEANO	Naval Oceanographic Office
NCEP	National Centers for Environmental Prediction
NDBC	National Data Buoy Center
netCDF	Network Common Data Format
NOAA	National Oceanographic and Atmospheric Administration
NOGAPS	Navy Operational Global Atmospheric Prediction System
NRL	Naval Research Laboratory
NWW3	NOAA Global WW3 model
OCF	Operational Consensus Forecast
OMB	Ocean Modeling Branch
PBS	Portable Batch System
pdf	probability distribution function
QuikSCAT	Quick Scatterometer
RMSE	Root Mean Square Error
ROAMER	Rapid Ocean Analysis Modeling Evaluation Relocatable
SAR	Synthetic Aperture Radar
SI	Scatter Index
SSM/I	Special Sensor Microwave/Imager
ST	Source Term package
SWAN	Simulating WAves Nearshore
SWH	Significant Wave Height
TC	Tolman and Chalikov (1996)
TOPEX	Ocean Topographic Experiment satellite
UKMO	United Kingdom Meteorological Office
UQ	Ultimate Quickest propagation scheme
VAG	An operational French numerical wave model
VTR	Validation Test Report
WAM	WAve Model
WE05	Woodcock and Engel, 2005
WMO	World Meteorological Organization
WNA	North Atlantic regional wave model
WW3	WAVEWATCH III®

APPENDIX A

WAVEWATCH III: Transition to Naval Operations

James D. Dykes and W. Erick Rogers
Naval Research Laboratory, Stennis Space Center, Mississippi
Corresponding author: james.dykes@nrlssc.navy.mil

1. Introduction

Knowledge of the sea state and thus the wave conditions is important for naval operations calling for real-time operational support of wave forecasts. Two operational centers have been providing such support [1]. Fleet Numerical Meteorology and Oceanography Center (FNMOC) in Monterey, California, produce and deliver wave forecasts covering large spatial and long time scales to support general operations. Naval Oceanographic Office (NAVOCEANO) at Stennis Space Center, Mississippi, provide small scale wave forecasts covering shorter intervals to support specific missions involving littoral waters and surf zones.

The Naval Research Laboratory (NRL) at Stennis Space Center has been the primary transition partner with NAVOCEANO for enabling technologies in wave forecasting for small [2] and intermediate scales [3][4]. And, in cooperation with National Centers for Environment Prediction, the larger scale WAVEWATCH III® (WW3) [5] model in its current state has been transitioned to FNMOC [6] with a newer version coming to both NAVOCEANO and FNMOC within this year.

To provide wave energy boundary conditions to smaller scale wave models such as SWAN (Simulating Waves Nearshore) [7], NAVOCEANO runs the WAM (WAve Model) [8] for a set of large scale domains around the world. Replacing the WAM, NRL is developing and testing a system that will implement the multi-grid model version of WW3 [9] at NAVOCEANO. In addition, NRL is providing upgrades to the system at FNMOC to include curvilinear gridded domains, particularly to cover the Arctic Ocean [10].

In this paper, WW3 is briefly described highlighting the characteristics of the multi-grid system as well as that of curvilinear grids. Then, the system at NAVOCEANO will be described and test results will be given.

2. Multi-grid Model

WW3 [11] is a third-generation wave model developed at NOAA/NCEP which employs a third-order numerical propagation scheme in order to control numerical diffusion of swell. The wave growth and dissipation source terms are allow more rapid wave growth under the influence of strong wind forcing than in previous wave models.

WW3 solves the spectral action density balance equation for wavenumber-direction spectra. The implicit assumption of these equations is that the wave field, water depth and surface current field vary on time and space scales that are much larger than the corresponding scales of a single wave. Furthermore, the propagation scheme used by the model is conditionally stable, which means that the model becomes inefficient with resolution finer than O(1 km).

The current public release version of WW3 is v3.14. The multi-grid model allows for the two-way communication of energy across domain boundaries. Typically, as it is with older versions of WW3 and with WAM, a host model passes wave energy through the boundary to a nest domain and whatever happens within the nest domain does not affect the host grid. This can have the effect of not allowing the

computational results with significant events of a high resolution model—potentially using better winds and better bathymetry—to be shared with the host and other regions. Figure 1 illustrates this.

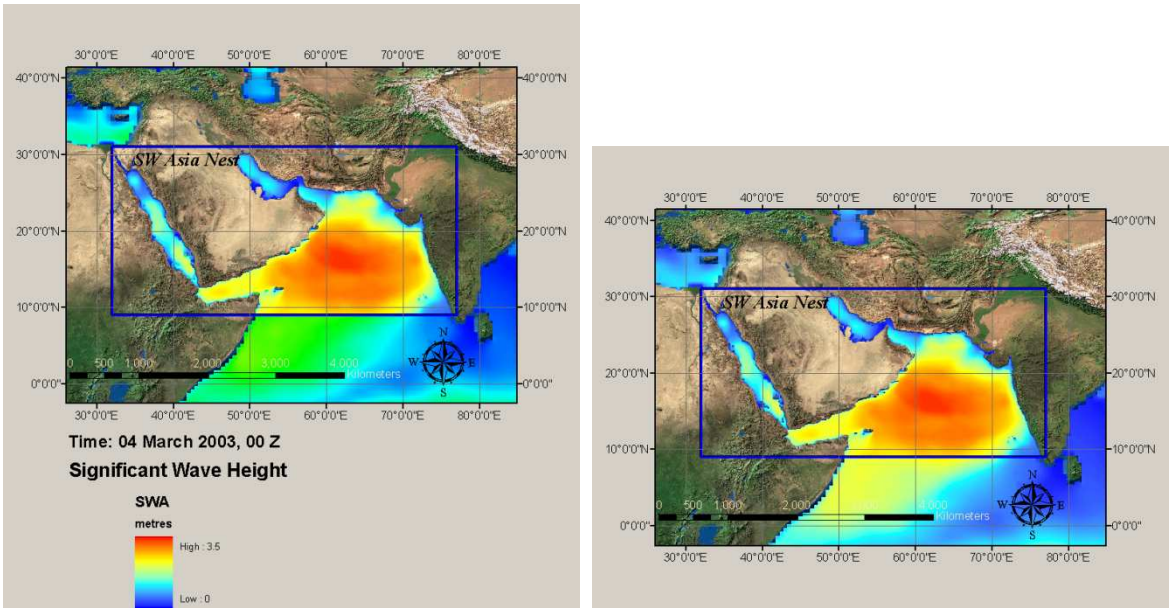

Figure 1: Example of a domain where in Panel a one-way nesting occurs, whilst results in Panel b are results from two-way nesting implemented in the multi-grid model.

An advantage to running the multi-grid version WW3 is that domain configuration is more efficient, using computational resources more where it is needed, i.e. minimizing the redundant use of computational resources. With older model versions, the model computed for all water points in the host domain regardless of whether these points were already covered by a nest. Now, the nest domain points are mutually exclusive from others except where there is overlap within the buffer zone around the boundaries. In addition, in a development version of the code (4.10), it is now possible that domains with different grid types (specifically curvilinear grids vs. regular grids) can be run together passing wave energy across the boundaries in both directions.

As the name implies, the multi-grid system runs multiple domains altogether instead of the traditional approach of running individual domains and passing boundary condition information to nest domains and running those separately. Since everything is together, the model set up is less tedious obviating the need to specify individual points in the host domain about the nest to which information is to be shared. One-way nesting is still available and is appropriate for small nests, which can be WW3 or other wave models such as SWAN.

3. Operational Implementation

NAVO has very specific requirements for how models are to run on their machines: specifically, requirements on timeliness of forecast products and the processing of data in the operational run-stream.

As soon as they are available wind fields from FNMOC arrive at NAVO and are processed to force the wave models. The arrival of the modelled wind fields is the primary factor that governs when any wave model can begin to run in any cycle. If it is certain that winds from a regional model such as the Coupled Ocean/Atmosphere Mesoscale Prediction System (COAMPS) [12] will arrive late, then the back-up plan is

to consider a different set of winds such as Navy Operational Global Atmospheric Prediction System (NOGAPS) [13] in order to maintain continuity between cycles.

On domains where it applies, ice concentrations from ice models such as the Polar Ice Prediction System (PIPS) [14] or the CICE model [15] can provide inputs to the model. Since, the ice field does not change significantly from one day to the next, it is not so critical to update the ice field daily in larger domains.

Restart files are used to maintain continuity between cycles. No model run for a cycle can start without either having a restart from a previous run, or by using a cold start (i.e. re-initializing with artificial conditions).

It gets a little more complicated for the system when running the multi-grid system. In this case all the wind fields from various meteorological models must be available before the multi-grid system can start. All the restarts in the system are made and used in tandem. For any one domain to be removed from the system a cold start must be implemented for all domains to continue, otherwise a void is left which the system cannot handle. Adding domains on the other hand can be done on the fly, since the energy of the original space over which the new domain is occupying is easily replaced with a cold start for that domain.

All models undergo some sort of pre- and post-processing with regards to the model run. This processing involves preparing the input data for the model run and taking the model output and converting it into other formats such as netCDF. For the multi-grid system, each individual domain can be processed before and after as if they were individual model runs. Links to files for the individual domains are used by the multi-grid system to access the files.

4. Transition to Operations

The wave forecast model system as has been described above is in the process of transition into operations. This means that the way NRL puts it together will be worked into the operational run stream at NAVO where operators will take over. Researchers at NRL and users at NAVO are coordinating the transition to best suit the needs of the operational customers.

A validation test report is provided to assure soundness of the model in typical scenarios. Some results of the validation are discussed below.

Once the model is installed in a way appropriate to operations, an operational evaluation and test are completed. In the operational test certain criteria that NAVO specifies must be met to consider the model ready for operations. The model being transitioned needs to meet and/or exceed the performance of existing capability.

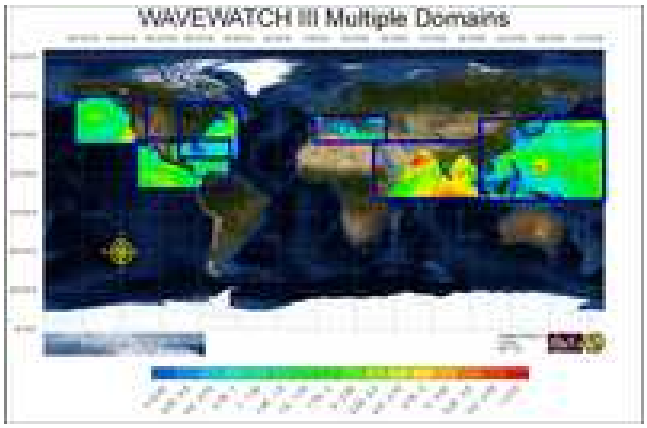

Figure 2: Global and regional domains used primarily for providing boundary conditions for smaller scale models.

5. Domain Coverage and Run Times

The current configuration for coverage of the world includes the globe at latitudinal and longitudinal grid spacing of 0.5 degrees and smaller domains at 0.2 and 0.1 degrees. Winds for the global domain come from NOGAPS, whilst the smaller domains are forced by COAMPS. The complete system (shown in Figure 2) as of this writing consists of a global domain and six regional domains.

In addition, in a development version of WW3 (v4.10), irregular grids are possible, and so the Arctic region can be covered by a curvilinear grid whose grid spacing is 16 km and has the additional input of ice concentration. A COAMPS grid covering the same regions provides the wind fields. The boundaries between the curvilinear and other grids behave just as was described earlier.

Many other areas surrounding the continents will be covered with a domain at 0.2 degrees grid spacing in order to provide the boundary conditions needed for small scale domains along many coasts. Except for the occasional coverage of COAMPS winds, most of these additional regions will be covered by NOGAPS.

The run cycles will almost always consist of runs every 12 hours, i.e. starting at 00 and 12 UST. Forecasts will run to at least 48 hours and potentially to 96 hours, depending on wind field availability.

The total wall time to run the system is quicker than the sum total of running the conventional individual runs. For a 48 hour forecast from start in the PBS to finish, the system wall clock time averaged about 1 hour and 13 minutes, where 64 processors were used.. This does not include the post processing as this could largely vary depending on the connectivity of the archive machine. Since the model scales very well, 256 processors may decrease the wall time by close to one fourth. The disadvantage to having the post-processing attached to the main run is that the latter process, though using only one processor, will cost the user all 64 (or 256) processor hours.

6. Preliminary Validation Results

Comparisons of both WAM and WW3 were made with in situ observations and altimeter measurements. For this paper, a buoy deployed into the waters of western Bermuda by the NOAA Data Buoy Center (NDBC), Buoy number 41048 located at 31°58'42" N 69°38'56" W was selected to evaluation the wave models at this location. Data and model runs for the time ranging from January through April were compiled. Results were plotted as time series, scatter plots, and wind roses. Table 1 shows a compilation of some of the results for TAU 00 (initial fields), including, mean bias (MB), standard deviation (SD), correlation coefficient (CC), slope(S) and scatter index (SI).

Table 1: Statistics from comparing NDBC Buoy 41048 to WAM and WW3 output.

Month	Model	MB	SD	CC	S	SI
Jan	WW3	-.27	.42	.93	.90	.17
	WAM	-.37	.43	.95	.82	.12
Feb	WW3	-.15	.35	.94	.94	.15
	WAM	-.32	.33	.96	.84	.11
Mar	WW3	-.21	.34	.90	.90	.15
	WAM	-.33	.37	.90	.82	.13
Apr	WW3	-.06	.33	.90	.82	.13
	WAM	-.28	.32	.93	.83	.12

Results from this buoy show that the mean bias for WW3 is always smaller than WAM, i.e. both wave models forecasts are low, but WAM is always lower.

7. Conclusion

Transition plans for WW3 are now underway. The multi-grid system will be an improvement to the current wave modelling systems in place at NAVO and FNMOC, because the new configuration will save processing time and promises to increase forecast accuracy. Preliminary validation results seem to bear this out.

8. Acknowledgement

Thanks go to Gretchen Dawson at NRL who processed the statistics.

9. References

[1] Jensen, R. E., P. A. Wittmann, and J. D. Dykes, Global and Regional Wave Modeling Activities: *Oceanography*, Vol 15, No. 1, 2002, pp. 57-66.

[2] R. A. Allard, J. D. Dykes**,** Y. L. Hsu, J. M. Kaihatu, and Dean Wakeham, 2008: A real-time Nearshore Wave and Current Prediction System. *J. of Marine Sys*, Vol. 69, Issues 1-2, January 2008, pp. 37-58

[3] J. D. Dykes, D.W. Wang, and J.W. Book, An evaluation of a high-resolution operational wave forecasting system in the Adriatic Sea. *J. of Marine Sys*, Vol. 78, Special Issue, January 2009, pp. 255-271

[4] W. E. Rogers, J. M. Kaihatu, L. Hsu, R. E. Jensen, J. D. Dykes, and K T. Holland, Forecasting and hindcasting waves with the SWAN model in the Southern California Bight, *Coastal Engineering*, Vol. 54, January 2007, 10-15.

[5] T. L. Tolman, B. Balasubtaminiyan, L. D. Burroughs, D. V. Chalikov, Y. Y. Chao, H. S. Chen, and V. M. Gerald, Development and implementation of wind generated ocean surface wave models at NCEP, *Wea, and Forecasting*, Vol. 17, April 2002, 311-333.

[6] P. A. Wittmann, Implementation of WW3 at Fleet Numerical Meteorology and Oceanography Center, *Ocean 2001, MTS/IEEE Conf.*, Honolulu, Hawai'i, 07 August 2002.

[7] N. Booij, R. C. Ris, and L.H. Holthuijsen, A Third-Generation Wave Model for Coastal Region: 1. Model Description and Validation, *J. Geophys. Res*. **104**(C4), 7649-7666.

[8] WAMDI Group, The WAM model—a third generation ocean wave prediction model. *J. Phys. Oceanogr*., **18** (1988), pp. 1775–1810

[9] H. L. Tolman, Toward a third release of WAVEWATCH III; a multi-grid model version, Tech. Note 251, NOAA/NWS/NCEP/MMAB, 2007, 12 pp.

[10] Rogers, W. E., and T. J. Campbell, 2009: Implementation of Curvilinear Coordinate System in the WAVEWATCH-III Model. *NRL Memorandum Report: NRL/MR/7320-09-9193*, 42 pp.

[11] H. Tolman and D. Chalikov, Source terms in a third generation wind-wave model, *J. of Phys. Oceanography*, 26, 1996, 2497-2518.

[12] Hodur, R. M., et al., The Coupled Ocean/ Atmosphere Mesoscale Prediction System (COAMPS), *Oceanography*, Vol 15, No. 1, 2002, pp. 88-98.

[13] Rosmond, T. E., J. Teixeira, M. Peng, T. F. Hogan, Navy Operational Global Atmospheric Prediction System (NOGAPS): Forcing for Ocean Models, *Oceanography*, Vol 15, No. 1, 2002, pp. 99-108.

[14] Van Woert, M. L., et al., Forecast Verification of the Polar Ice Prediction System (PIPS) Sea Ice Concentration Fields. *J. Atmos. Oceanic Technol.*, Vol 21, pp. 944–957.

[15] Hunke, E. C., and W. H. Lipscomb, CICE: The Los Alamos sea ice model, Documentation and software, version 3. Tech. Report LA-CC-98-16, Los Alamos National Laboratory, Los Alamos, NM, 52 pp.

APPENDIX B

Here resides the table of all the buoys addressed in this report. All of these buoy locations can easily be found on the NDBC web site by simply typing in the buoy number in the search box. Files from the historical archives can be downloaded and unzipped for immediate access.

Table B-1: Depth and location of NDBC buoys used in model validation. The section(s) of this report in which some buoys were used is also indicated.

NDBC Buoy	Water Depth (m)	Distance from shore	Latitude	Longitude	Section used in
41001	4462.3	150 NM E of Cape Hatteras	34.68 N	72.66 W	4
41010	876.6	120 NM E of Cape Canaveral	28.89 N	78.52 W	4
41048	5261	240 NM West of Bermuda	31.98 N	69.50 W	3, 4
41049	5456	300 NM SSE of Bermuda	27.50 N	63.01W	
42059	4785	190 NM NNE of Curacao	15.05 N	67.47 W	
42036	54.5	106 NM WNW of Tampa FL	28.50 N	84.52 W	3
42040	164.6	64 NM South of Dauphin Island AL	28.21 N	87.21 W	
44005	206	78 NM East of Portsmouth NH	43.20 N	69.13 W	
44008	64.8	54 NM Southeast of Nantucket	40.50 N	69.25 W	
46002	3444	275 NM West of Coos Bay OR	42.59 N	130.47 W	
46005	2981	315 NM West of Aberdeen WA	46.10 N	132.00 W	
46006	4151.4	600 NM W of Eureka CA	40.75 N	137,46 W	4
46015	420.3	16 NM West of Port Orford OR	42.76 N	124.83 W	
46022	674.8	17 NM WSW of Eureka CA	40.72 N	124.58 W	
46025	905.3	33 NM WSW of Santa Monica CA	33.75 N	119.05 W	
46028	1158.2	55 NM WNW of Morro Bay CA	35.74 N	121.88 W	3
46029	144.8	20 NM W of Columbia River Mouth	36.75 N	134.51 W	
46042	2098	27 NM West of Monterey Bay	36.79 N	122.57 W	
46047	1399	121 NM West of San Diego CA	32.40 N	119.54 W	
46050	128	20 NM West of Newport OR	44.62 N	124.53 W	
46089	2289	85 NM WNW of Tillamook OR	45.89 N	125.83 W	
46246	4253	Ocean Station PAPA	49.99 N	145.09 W	

APPENDIX C

The following are supplemental statistics following along the same idea as described in Section 3 regarding the statistics of model to buoy observation comparisons described there. The 00-hour results are included but not the 24-hour since the main issue is the model response to the wind forcing which is the dominant factor in the case of the 24-hour forecast for this configuration. The number of sample points is between 55 and 62 mainly depending on the month. Model domain names for both WAM and WW3 are indicated. The domains of the WW3 are described in Section 3.1.

Table C-1: Summary statistics for WW3 and WAM output within domains *w_atl_n2* and *w_atl_nest2_appl*, respectively, compared to NDBC buoys indicated by section.

Month in 2011	MB [WW3]	MB [WAM]	RMSD [WW3]	RMSD [WAM]	CC [WW3]	CC [WAM]	Slope [WW3]	Slope [WAM]	SI [WW3]	SI [WAM]
150 NM East of Cape Hatteras (NDBC 41001)										
Jan	-0.36	-0.37	0.57	0.58	0.93	0.94	0.82	0.73	0.24	0.24
Feb	-0.38	-0.46	0.56	0.59	0.93	0.95	0.83	0.79	0.22	0.23
Mar	-0.33	-0.40	0.50	0.54	0.88	0.89	0.83	0.66	0.22	0.23
Apr	-0.21	-0.38	0.49	0.56	0.89	0.94	0.75	0.66	0.22	0.25
240 NM West of Bermuda (NDBC 41048)										
Jan	-0.34	-0.22	0.52	0.44	0.85	0.88	0.66	0.61	0.30	0.26
Feb	-0.18	-0.32	0.39	0.42	0.95	0.97	1.00	0.83	0.17	0.19
Mar	-0.18	-0.30	0.36	0.42	0.92	0.93	1.02	0.72	0.17	0.19
Apr	-0.07	-0.28	0.31	0.38	0.90	0.94	0.95	0.73	0.17	0.20
78 NM East of Portsmouth, New Hampshire (NDBC 44005)										
Jan	-0.58	-0.20	0.71	0.47	0.92	0.90	0.71	0.81	0.43	0.28
Feb	-0.53	-0.20	0.65	0.46	0.89	0.87	0.78	0.91	0.34	0.25
Mar	-0.48	-0.31	0.63	0.59	0.86	0.78	0.72	0.58	0.32	0.30
Apr	-0.31	-0.17	0.56	0.54	0.87	0.85	0.79	0.65	0.32	0.30
54 NM Southeast of Nantucket (NDBC 44008)										
Jan	-0.49	-0.36	0.65	0.56	0.95	0.95	0.78	0.76	0.31	0.26
Feb	-0.35	-0.34	0.56	0.55	0.94	0.94	0.81	0.82	0.23	0.23
Mar	-0.20	-0.25	0.44	0.45	0.87	0.88	0.83	0.71	0.22	0.22
Apr	-0.13	-0.38	0.43	0.56	0.92	0.93	0.98	0.71	0.20	0.26

Table C-2: Summary statistics for WW3 and WAM output within domains *centam_n2* and *cent_am_nest2_appl*, respectively, compared to NDBC buoys indicated by section.

Month in 2011	MB [WW3]	MB [WAM]	RMSD [WW3]	RMSD [WAM]	CC [WW3]	CC [WAM]	Slope [WW3]	Slope [WAM]	SI [WW3]	SI [WAM]
120 NM East of Cape Canaveral (NDBC 41010)										
Jan	-0.34	-0.29	0.52	0.51	0.85	0.86	0.65	0.53	0.30	0.30
Feb	-0.26	-0.24	0.42	0.39	0.69	0.76	0.51	0.45	0.28	0.26
Mar	-0.25	-0.28	0.41	0.40	0.88	0.90	0.98	0.65	0.24	0.24
Jul	-0.16	-0.14	0.24	0.23	0.89	0.89	0.92	0.64	0.20	0.20
300 NM SSE of Bermuda (NDBC 41049)										
Jan	-0.46	-0.33	0.60	0.57	0.85	0.76	0.84	0.48	0.27	0.26
Feb	-0.28	-0.27	0.52	0.40	0.88	0.95	0.95	0.83	0.24	0.18
Mar	-0.32	-0.33	0.47	0.41	0.87	0.95	0.97	0.65	0.22	0.19
Jul	-0.29	-0.19	0.34	0.24	0.61	0.68	0.63	0.56	0.27	0.19
106 NM West of Tampa, Florida (NDBC 42036)										
Jan	-0.29	-0.29	0.44	0.45	0.85	0.84	0.70	0.61	0.39	0.40
Feb	-0.27	-0.25	0.39	0.39	0.85	0.84	0.70	0.58	0.49	0.49
Mar	-0.20	-0.22	0.28	0.29	0.92	0.93	0.93	0.75	0.35	0.36
Jul	-0.19	-0.12	0.29	0.20	0.80	0.81	1.06	0.75	0.56	0.39
64 NM South of Dauphin Island, Alabama (NDBC 42040)										
Jan	-0.14	-0.17	0.46	0.50	0.80	0.78	0.66	0.54	0.40	0.42
Feb	-0.11	-0.14	0.42	0.44	0.72	0.68	0.64	0.50	0.46	0.48
Mar	-0.10	-0.20	0.38	0.45	0.87	0.84	0.86	0.61	0.36	0.42
Jul	-0.16	-0.07	0.25	0.18	0.77	0.74	0.92	0.61	0.48	0.35
190 NM NNE of Curacao (NDBC 42059)										
Jan	-0.16	-0.12	0.34	0.29	0.80	0.83	0.81	0.63	0.17	0.15
Feb	-0.18	-0.05	0.35	0.32	0.83	0.75	0.97	0.58	0.17	0.16
Mar	-0.12	-0.03	0.25	0.24	0.79	0.76	0.73	0.48	0.16	0.15
Jul	-0.21	-0.29	0.31	0.37	0.82	0.75	0.95	0.59	0.19	0.23

Table C-3: Summary statistics for WW3 and WAM output within domains *e_pac_n2* and *e_pac_nest2_appl*, respectively, compared to NDBC buoys indicated by section.

Month in 2011	MB [WW3]	MB [WAM]	RMSD [WW3]	RMSD [WAM]	CC [WW3]	CC [WAM]	Slope [WW3]	Slope [WAM]	SI [WW3]	SI [WAM]
275 NM West of Coos Bay, Oregon (NDBC 46002)										
Jun	+0.17	+0.47	0.26	0.57	0.91	0.72	0.89	0.61	0.15	0.35
Jul	+0.16	+0.48	0.28	0.54	0.81	0.70	0.91	0.67	0.17	0.33
Aug	+0.12	+0.59	0.23	0.64	0.81	0.63	0.65	0.33	0.18	0.48
315 NM West of Aberdeen, Washington (NDBC 46005)										
Jun	+0.16	+0.48	0.27	0.60	0.91	0.73	0.77	0.53	0.17	0.37
Jul	+0.18	+0.40	0.32	0.51	0.81	0.68	0.94	0.69	0.20	0.31
600 NM West of Eureka, California (NDBC 46006)										
Apr	+0.27	+0.05	0.46	0.49	0.91	0.88	0.87	0.53	0.17	0.18
May	+0.05	+0.03	0.33	0.41	0.92	0.86	0.88	0.53	0.14	0.18
Jun	+0.22	+0.53	0.29	0.58	0.88	0.80	0.80	0.66	0.19	0.38
Jul	+0.10	+0.45	0.24	0.53	0.89	0.76	0.87	0.60	0.15	0.33
Aug	+0.13	+0.51	0.25	0.58	0.88	0.84	0.72	0.45	0.18	0.42
16 NM West of Port Orford, Oregon (NDBC 46015)										
May	+0.08	+0.37	0.34	0.45	0.74	0.85	0.67	0.75	0.17	0.23
Jun	+0.18	+0.52	0.31	0.62	0.83	0.67	0.70	0.46	0.20	0.40
Aug	+0.27	+0.65	0.42	0.74	0.57	0.49	0.42	0.38	0.31	0.55
17 NM WSW of Eureka, California (NDBC 46022)										
Apr	+0.16	+0.09	0.37	0.53	0.94	0.88	0.84	0.53	0.15	0.21
May	+0.05	+0.29	0.42	0.51	0.71	0.72	0.59	0.55	0.21	0.25
Jun	+0.26	+0.53	0.46	0.68	0.88	0.87	0.71	0.57	0.24	0.36
33 NM WSW Santa Monica, California (NDBC 46025)										
Apr	-0.21	+0.72	0.49	0.84	0.16	0.36	0.15	0.41	0.38	0.65
May	-0.12	+0.84	0.35	0.91	0.78	0.86	0.59	1.07	0.59	0.69
Jun	+0.25	+1.00	0.34	1.04	0.62	0.65	0.51	0.86	0.34	1.04
Jul	+0.08	+1.00	0.33	1.04	0.70	0.77	1.45	1.57	0.36	1.12
Aug	+0.10	+0.83	0.27	0.85	-0.30	0.12	-0.22	0.09	0.27	0.86
55 NM WNW of Morro Bay (NDBC 46028)										
Apr	-0.34	+0.05	0.66	0.62	0.89	0.87	0.58	0.51	0.25	0.24
May	-0.17	+0.32	0.44	0.53	0.74	0.73	0.62	0.71	0.19	0.23
Jun	+0.05	+0.47	0.34	0.59	0.81	0.77	0.69	0.62	0.16	0.28
Jul	+0.38	+0.64	0.57	0.89	0.59	0.13	0.49	0.11	0.31	0.49
Aug	+0.21	+0.66	0.36	0.71	0.76	0.84	0.51	0.57	0.21	0.41

Table C-3 continued.

Month in 2011	MB [WW3]	MB [WAM]	RMSD [WW3]	RMSD [WAM]	CC [WW3]	CC [WAM]	Slope [WW3]	Slope [WAM]	SI [WW3]	SI [WAM]
20 NM Columbia River Mouth (NDBC 46029)										
Apr	+0.19	+0.05	0.39	0.47	0.94	0.89	1.03	0.59	0.15	0.18
May	+0.03	+0.25	0.31	0.41	0.80	0.73	0.86	0.61	0.17	0.22
Jun	+0.14	+0.47	0.25	0.57	0.90	0.74	0.81	0.50	0.17	0.39
Jul	+0.20	+0.52	0.36	0.66	0.52	0.06	0.47	0.05	0.25	0.46
Aug	+0.16	+0.56	0.26	0.62	0.85	0.77	0.64	0.77	0.22	0.52
27 NM West of Monterey Bay (NDBC 46042)										
Apr	-0.43	+0.18	0.70	0.51	0.89	0.90	0.48	0.60	0.30	0.22
May	-0.40	+0.23	0.55	0.47	0.80	0.76	0.56	0.64	0.25	0.22
Jun	-0.23	+0.36	0.53	0.62	0.76	0.70	0.41	0.43	0.25	0.30
Jul	+0.22	+0.48	0.54	0.78	0.55	0.18	0.46	0.12	0.29	0.43
Aug	+0.08	+0.70	0.24	0.74	0.69	0.66	0.47	0.50	0.16	0.50
121 NM West of San Diego, California (NDBC 46047)										
Apr	+0.40	+0.42	0.63	0.67	0.77	0.69	0.78	0.48	0.28	0.30
May	+0.25	+0.47	0.55	0.65	0.70	0.74	0.77	0.78	0.25	0.30
Jun	+0.32	+0.58	0.57	0.75	0.43	0.40	0.46	0.41	0.31	0.41
Jul	+0.32	+0.61	0.46	0.72	0.53	0.50	0.76	0.77	0.26	0.41
Aug	+0.27	+0.51	0.37	0.58	0.70	0.64	0.54	0.37	0.21	0.33
20 NM West of Newport, Oregon (NDBC 46050)										
Apr	-0.08	-0.15	0.53	0.64	0.87	0.88	0.79	0.47	0.19	0.23
May	-0.13	+0.15	0.37	0.40	0.77	0.72	0.73	0.57	0.19	0.20
Aug	+0.09	+0.53	0.23	0.60	0.79	0.65	0.64	0.39	0.18	0.46
85 NM WNW of Tillamook, Oregon (NDBC 46089)										
Apr	+0.39	+0.21	0.53	0.50	0.95	0.89	1.08	0.62	0.21	0.20
May	+0.11	+0.28	0.34	0.45	0.79	0.69	0.88	0.60	0.18	0.24
Jun	+0.23	+0.51	0.32	0.61	0.91	0.80	0.88	0.60	0.21	0.39
Jul	+0.22	+0.52	0.37	0.65	0.59	0.29	0.59	0.26	0.25	0.44
Aug	+0.24	+0.63	0.30	0.67	0.85	0.76	0.82	0.51	0.24	0.54
Ocean Station PAPA (NDBC 46246)										
Apr	+0.15	-0.26	0.51	0.70	0.97	0.98	0.95	0.69	0.15	0.21
May	-0.09	-0.25	0.39	0.46	0.89	0.91	0.86	0.63	0.14	0.16
Jun	+0.09	+0.26	0.37	0.47	0.82	0.81	0.66	0.48	0.21	0.26
Jul	+0.21	+0.26	0.43	0.45	0.83	0.76	1.01	0.61	0.21	0.22
Aug	+0.14	+0.25	0.28	0.44	0.95	0.92	0.94	0.59	0.16	0.25